

**STUDY ON MAGNETOHYDRODYNAMICS NANOFLUID
FLOW THROUGH EXPANDING OR CONTRACTING
CHANNEL WITH PERMEABLE WALLS**

By

MD. KHALILUR RAHMAN

Roll No. 0413093009P,

Registration No. 0413093009, Session: April 2013

Master of Philosophy
in
Mathematics



Department of Mathematics

BANGLADESH UNIVERSITY OF ENGINEERING AND TECHNOLOGY

DHAKA-1000

25 February-2018

This thesis entitled

**STUDY ON MAGNETOHYDRODYNAMICS NANOFLUID FLOW
THROUGH EXPANDING OR CONTRACTING CHANNEL WITH
PERMEABLE WALLS**

Submitted By

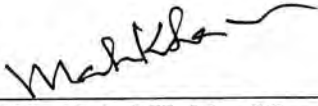

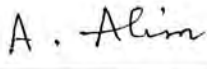
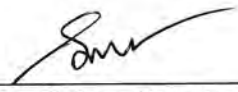
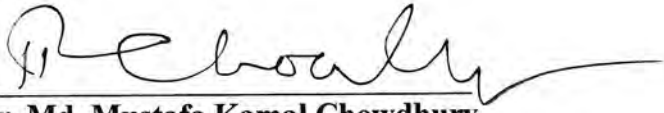
Md. Khalilur Rahman

Roll No: 0413093009(Part time), Registration No: 0413093009, Session: April 2013 has been
accepted as satisfactory in partial fulfillment of the requirement for the degree of

Master of Philosophy in Mathematics

On 25 February 2018

Board of Examiners

- (i) 
Dr. Md. Abdul Hakim Khan (Supervisor) Chairman
Professor
Department of Mathematics, BUET, Dhaka.
- (ii) 
Head (Ex-Officio) Member
Department of Mathematics, BUET, Dhaka.
- (iii) 
Dr. Md. Abdul Alim Member
Professor
Department of Mathematics, BUET, Dhaka.
- (iv) 
Dr. Salma Parvin Member
Professor
Department of Mathematics, BUET, Dhaka.
- (v) 
Dr. Md. Mustafa Kamal Chowdhury Member
Professor (Retd.) (External)
Department of Mathematics, BUET, Dhaka.
Address: 110, Lake Garden, Lake Circus Road, Kalabagan, Dhaka.

Dedication

To My Heartiest Daughter

Kafifa Juwairiya (Radia)

Author's Declaration

I hereby declare that the work in this thesis was carried out in accordance with the regulations of the Bangladesh University of Engineering and Technology. The work is original except where indicated by special reference in the text and no part of the dissertation has been submitted for any other degree at any university or institution other than publications.



Md. Khalilur Rahman

25 February 2018

Acknowledgement

First of all I want to express my gratefulness to Almighty Allah, the most merciful, benevolent to mankind, for enabling me to complete the work successfully.

I have the privilege to express my deep respect, gratitude and sincere appreciation to my supervisor Professor **Dr. Md. Abdul Hakim Khan**, Department of Mathematics, Bangladesh University of Engineering and Technology, Dhaka, who initiated me into the realm of mathematical research. Without his valuable guidance, constant encouragement and generous help it would have been difficult to complete this thesis. I am grateful to him for giving me the opportunity to work with him as a research student and for every effort that he made to get me on the right track of this thesis.

I wish to express my gratitude to Professor **Dr. Md. Mustafa Kamal Chowdhury**, Professor **Dr. Md. Abdul Alim** and Professor **Dr. Md. Mustafizur Rahman**, Head, Department of Mathematics, Bangladesh University of Engineering and Technology, for their guidance, encouragement and providing all necessary help in the department. I would like to extend my sincere thanks to all other respected teachers of the Department of Mathematics, BUET.

I express my gratitude to all members of the Board of examiner Professor Dr. Md. Mustafa Kamal Chowdhury, Professor Dr. Md. Abdul Alim, Professor Dr. Salma Parvin and Professor Dr. Md. Mustafizur Rahman, Head, Department of Mathematics, Bangladesh University of Engineering and Technology.

My sincere thanks to my colleagues and the authority of my institution for providing me necessary support and facilities during my research works.

It is impossible to express in words my indebtedness to my daughter Kafifa Juwairiyah (Radiya) and wife Jobaida Akter for their sacrifice, assistance and motivation during the preparation of thesis work. I must acknowledge my debt to my parents for whom I have been able to see the beautiful sights and sounds of the world.

Abstract

The present study investigates the influence of external magnetic field on unsteady incompressible flow of water-based nanofluid through a successively expanding or contracting channel with porous walls. The basic governing equations with boundary conditions are non-dimensionalized using appropriate transformation to ordinary differential equations, which are then being bifurcation diagrams of velocity field and wall shear stress are gained which signifies the stability of the flow. The regular effects of the different governing physical parameters specifically Hartmann number, volume fraction of nanoparticles, non-dimensional wall dilation rate and permeable Reynolds number on velocity profiles are depicted graphically.

This research work also investigates the influence of external magnetic field on unsteady incompressible flow of water based different nanofluid (Cu,Ag,Al₂O₃) through a successively expanding or contracting channel with porous walls.

This research shows the stability of the flow through bifurcation diagram of velocity versus non-dimensional wall dilation rate.

Contents	Page No
Board of Examiners	i
Acknowledgement	iii
Acknowledgement	iv
Abstract	v
Nomenclature	viii
List of Table	ix
List of Figures	x
Chapter 1: Introduction	
1.1: Fluid	1
1.2: Magneto hydrodynamics (MHD)	1
1.3: Application of MHD	3
1.4: Nanofluids	3
1.5: Application of Nanofluids	4
1.6: Nanoparticles solid volume fraction	5
1.7: Channel Flow	6
1.8: Power series	7
1.9: Singularity analysis	8
1.10: Elementary bifurcation Theory	10
1.11: Literature review	11
1.12: Objectives of this thesis	13
1.13: Organization of Thesis	14
Chapter 2: Approximation Methods	
2.1: Introduction	15
2.2: Hermite- Padé approximants	15
2.3: Padé Approximants	17
2.4: Algebraic approximants	19
2.5: Drazin-Tourigney Approximants	21
2.6: Differential Approximants	21

2.7: High Order Differential Approximants (HODA)	23
2.8: High-Order Partial Differential Approximants (HPDA)	24
Chapter 3: Governing Equations of The Problem	
3.1: Introduction	26
3.2: Continuity Equation	26
3.3: Momentum Equation (Navier-Stokes Equation)	27
3.4: The Governing equations in Cartesian coordinate system	27
3.5: The Governing equations in Cylindrical coordinate system	28
3.6: M ' Eq	29
3.7: General Equations Governing Magnetohydrodynamic Nanofluid flow	30
3.7.1: The Continuity Equation	30
3.7.2: The Momentum (Navier-Stokes) Equation	30
Chapter 4: Magnetohydrodynamics Nanofluid Flow through Expanding or Contracting	
 Channel with Permeable Walls	
4.1: Introduction	32
4.2: Mathematical configuration	33
4.3: Physical Properties	34
4.4: Mathematical Formulation	34
4.5: Series Analysis	36
4.6: Results and Discussion	37
4.7: Special Case	47
4.8: Bifurcation	67
4.9: Conclusion	68
Chapter 5: Conclusions	
5.1: Conclusion	69
5.2: Possible future works based on this thesis	70
Reference	71

Nomenclature

B_0	Magnetic field intensity
f'	Dimensionless Velocity
Ha	Hartmann Number
Re	Permeable Reynolds Number
\bar{p}	Dimensional Pressure of the fluid
t	Time
$a(t)$	Height of the channel from origin
\bar{u}, \bar{v}	Velocity components along x, y-axis
\bar{V}_w	Injection velocity
\bar{x}, \bar{y}	Cartesian Co-ordinates

Greek symbols

μ	Dynamic viscosity of the fluid
ν	Kinematic viscosity
α	Non-dimensional wall dilation rate
τ	Shear stress
ρ	Fluid density
σ	Electrical conductivity of the fluid
ψ	Dimensionless Stream function
ϕ	Solid volume fraction

Subscripts

∞	Condition at infinity
nf	Nanofluid
f	Base fluid
s	Solid particles

Superscripts

Prime (') differentiation with respect to y

List of Table

Page No

Table: 2.1 Approximant of x_c by Padé for the function in example 2.1	18
Table: 2.2 Approximation of x_c by algebraic approximant for the function of ex.2.2.	20
Table: 2.3 Approximation of x_c by differential approximant for the function of ex.2.3.	23
Table: 4.1 Thermo physical properties of different nanoparticles and base water.	34
Table: 4.2 Significant difference among different value Φ for Cu -nanofluid.	51
Table: 4.3 S c c Φ for Ag- nanofluid.	56
Table: 4.4 S c c Φ for Al_2O_3 -nanofluid.	61
Table: 4.5 Significant Comparison of Stability for Different MHD Nanofluid:	66

List of Figure	Page No
Fig:- 1.1 Magnetohydrodynamics (MHD)	2
Fig:- 1.2 Nanofluid	4
Fig:- 1.3 Porous channel	6
Fig:- 4.1 Physical configuration of the problem.	33
Fig:- 4.2(a) Non-dimensional wall dilation rate effect on stream function and comparison.	38
Fig:- 4.2(b) Non-dimensional wall dilation rate effect on velocity profile and comparison.	39
Fig:- 4.3(a) Nanoparticles volume fraction effect on stream function and comparison.	40
Fig:- 4.3(b) Nanoparticles volume fraction effect on velocity profile and comparison.	41
Fig:- 4.4(a) Reynolds number effect on stream function and comparison.	42
Fig:- 4.4(b) Reynolds number effect on velocity profile and comparison.	43
Fig:- 4.5(a) Nanoparticles volume fraction effect on stream function and comparison.	44
Fig:- 4.5(b) Nanoparticles volume fraction effect on velocity profile and comparison.	45
Fig:- 4.6 Shear stress for different parameters.	46
Fig:- 4.7(A)-1 (a) Stream function (b) Velocity profile (c) Shear stress for cu- water based nanofluid flow for different value of α W $R = 1$; $\beta = 1, 2$; $\Phi = 0.04$.	47
Fig:- 4.7(A)-2 (a) Stream function (b) Velocity profile (c) Shear stress for cu- water based W $R = 1$; $\alpha = 1$; $\Phi = 0.04$	48
Fig:- 4.7(A)-3 (a) Stream function (b) Velocity profile (c) Shear stress for cu- water based R W $\alpha = 1$; $\beta = 1, 2$; $\Phi = 0.04$	49
Fig:- 4.7(A)-4 (a) Stream function (b) Velocity profile (c) Shear stress for cu- water based Φ W $\alpha = 1$; $\beta = 1, 2$; $Re = 1$.	50
Fig:- 4.7(B)-1 (a) Stream function (b) Velocity profile (c) Shear stress for Ag - water based nanofluid flow for different value of α W $\Phi = 0.04$; $\beta = 1, 2$; $Re = 1, 4$.	52

Fig:- 4.7(B)-2 (a) Stream function (b) Velocity profile (c) Shear stress for Ag - water based nanofluid flow for different value of Ha	W	$\alpha = 1$; $R = 1, 4$; $\Phi = 0.04$	53	
Fig:- 4.7(B)-3 (a) Stream function (b) Velocity profile (c) Shear stress for Ag – water based	R	W	$\alpha = 1$; $\beta = 1$; $\Phi = 0.04$	54
Fig:- 4.7(B)-4 (a) Stream function (b) Velocity profile (c) Shear stress for Ag – water based nanofluid flow for different value of Φ	W	$\alpha = 1$; $Re = 1$; $Ha = 1$.	55	
Fig:- 4.7(C)-1(a) Stream function (b) Velocity profile (c) Shear stress for Al_2O_3 -water based	α	W	$\Phi = 0.04$; $\beta = 1$; $R = 1$	57
Fig:- 4.7(C)-2(a) Stream function (b) Velocity profile (c) Shear stress for Al_2O_3 - water based nanofluid flow for different value of Ha	W	$\alpha = 1$; $R = 1$; $\Phi = 0.04$	58	
Fig:- 4.7(C)-3 (a) Stream function (b) Velocity profile (c) Shear stress for Al_2O_3 - water based	R	W	$\alpha = 1$; $\beta = 1$; $\Phi = 0.04$	59
Fig:- 4.7(C)-4 (a) Stream function (b) Velocity profile (c) Shear stress for Al_2O_3 - water based	Φ	W	$\alpha = 1$; $Ha = 1$; $Re=1$.	60
Fig:- 4.7(D)-1 (a) Stream function (b) Velocity profile (c) Shear stress with absence of	α	W	$\beta = 1, 2$; $Re= 1, 4$; $\Phi=0.04$	62
Fig:- 4.7(D)-2(a) Stream function (b) Velocity profile (c) Shear stress with absence of	W	$\alpha = 1$; $R = 1, 4$; $\Phi=0.04$	63	
Fig:- 4.7(D)-3 (a) Stream function (b) Velocity profile (c) Shear stress with absence of	R	W	$\alpha = 1$; $\beta = 1, 2$; $\Phi=0.04$	64
Fig:- 4.7(E)(a) Stream function (b) Velocity profile (c) Shear stress for different nanofluid	W	$\alpha = 1$; $\beta = 1, 2$; $Re=1, 4$; $\Phi=0.04$	65	
Fig:-4.8: Bifurcation diagram of velocity at the porous wall for Cu-water nanofluid.			67	

INTRODUCTION

1.1 Fluid

A fluid is any substance that deforms continuously when subjected to a shear stress (tangential force per unit area), no matter how small according to Mc Donough. Though the work of Leonardo Da Vinci gave rapid advancement to the study of fluid mechanics more than 500 years ago, fluid behavior were much more available by the time of ancient Egyptian. Enough practical information had been gathered during the Roman Empire to allow fluid dynamics application. More modern understanding of fluids motion was begun through Bernoulli's equation several centuries ago,. Since then, many researchers have done numerous works on fluid mechanics.

The study of fluid flowing through a porous channel fascinated mankind for many centuries due to its applications in many areas of life. Such areas are: agriculture (e.g. irrigation, land drainage), geothermal system, micro-electric heat transfer equipment, coal and grain storage, nuclear waste disposal, hydraulic engineering, atmospheric sciences, oceanography, geophysics (e.g. convection in earth's mantle, convection in earth's molten area). So, also in chemical and petroleum engineering (e.g. industrial filtration, fluidization, sedimentation, metallurgy, ceramics, powders, drying and wetting of textiles and wood), building engineering and biological area (e.g. flow of the blood and water system, action of kidney and rise of juices in plant).

However, the flow of an electrically conducting viscous fluid between two parallel in the presence of a transversely applied magnetic field has an application in many devices such as magneto hydrodynamics (MHD) powers generators.

1.2 Magnetohydrodynamics (MHD)

The term MHD is comprised of the words magneto- means magnetic, hydro- means fluids, and dynamics- means movement. It is the branch concern with the dynamics of electrically conducting fluid in magnetic field. These fluids include salt water, liquid metals (such as Mercury, gallium, molten Iron) and ionized gases or plasmas (such as solar atmosphere). The field of MHD was initiated by Swedish Physicist Hannes Alfvén(1908-1995), who received the

noble prize in Physics in 1970 for fundamental works and discoveries in magnetohydrodynamics with different parts of plasma physics.

Magnetohydrodynamics exhibits the phenomena, where, in an electrically conducting field, the velocity field \underline{V} and the magnetic field \underline{B} are coupled. The magnetic field induces an electric current of density \underline{J} in the moving conductive fluid. The induced current creates forces on the liquid and changes the magnetic field \underline{B} experience and MHD force $\underline{J} \times \underline{B}$ known as Lorentz force. This Lorentz force tends to oppose the fluid motion near the edge. As the velocity is very small, the magnetic force that is proportional to the magnitude of the longitudinal velocity and acts in opposite direction is also very small. The set of equations that describe MHD flow are a combination of Navier-Stokes equation of Fluid dynamics and Maxwell's equation of electromagnetism.

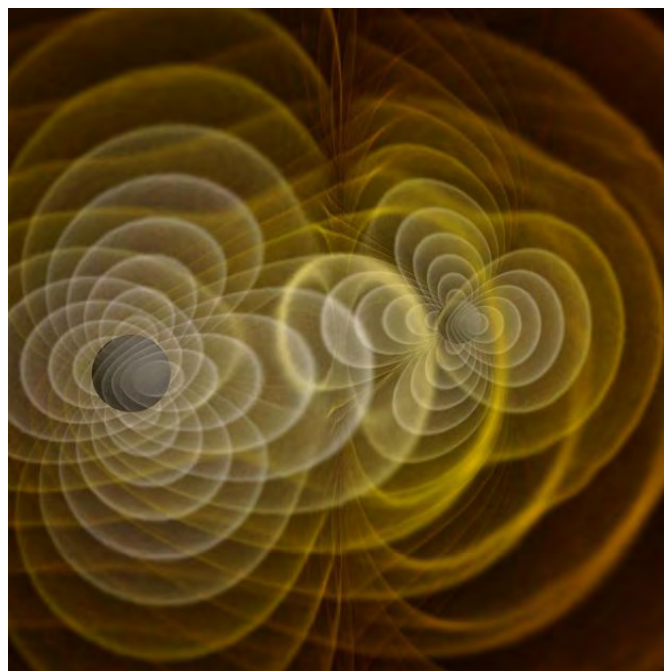


Fig:- 1.1 Magnetohydrodynamics(MHD) [Ref: Secrets-of-merging-black-holes-4]

1.3 Application of MHD

Many natural phenomena and engineering problems are susceptible to MHD analysis. In natural phenomena, since magnetic field exists everywhere in the world, it follows that MHD phenomena which must occur whenever conducting fluid are available.

Some common applications are: -

- Geothermal system
- Micro-electric heat transfer equipment
- Atmospheric sciences
- chemical and petroleum engineering
- Defence and Space applications
- Thermal storage
- Bio-medical applications
- Drilling and lubrications

1.4 Nanofluids

Nanofluids is a term coined by Choi in 1995 of the Argonne National Laboratory, U.S.A. (diameter less than 50nm). Nanofluids indicate Fluids with nanoparticles suspended in them. Suspended nanoparticles in the various base fluids can alter the fluid flow and heat transfer characteristics of the base fluids.

Some experimental studies have revealed that the nanofluids have remarkably higher thermal conductivities than those of conventional pure fluids and have great potential for heat transfer enhancement. Nanofluids are more suited for practical application than existing techniques for enhancing heat transfer by adding millimeter and/or micrometer-sized particles in fluids since nanofluids incur little or no penalty in pressure drop. Because the nanoparticles are so small

(usually less than 100nm) that they behave like a pure fluid without any particles in it. In addition, nanoparticles are less likely to cause wear because of their small sizes.

Nanofluids are a class of heat transfer fluids that have many advantages. They have better stability compared to those fluids containing micro- or mille-sized particles; moreover, they have higher thermal transfer capability than their base fluids. Such advantages offer important benefits for numerous applications in many fields such as transportation, heat exchangers, electronics cooling, nuclear systems cooling, biomedicine and food of many types. For example, in cooling systems, a 50/50 ethylene glycol (EG) and water mixture is commonly used as an automotive coolant. The mixture is a relatively poor heat transfer fluid compared to pure water. Water/EG mixtures with additional nanoparticles are currently being studied to enhance heat transfer performance. Nanoparticles can improve the heat transfer coefficient of pure ethylene glycol. Therefore, the resulting nanofluid performs better at low pressure working conditions and smaller coolant system size when compared to the 50/50 mixture. Finally, smaller and lighter radiators can be used to increase engine performance and fuel efficiency. Nanofluids can significantly reduce the thermal resistance of the heat pipe when compared to conventional demonized water.

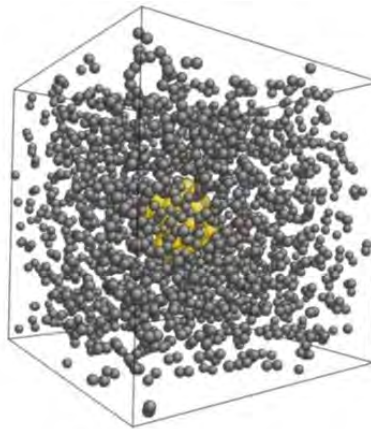


Figure 1.2: Nanofluid [ref: Net collection (pitt.edu)]

1.5 Application of Nanofluids

Nanofluids can be used to cool automobile engines and welding equipments and to cool high heat flux device such as high power microwave tubes, and high power laser diode array. Nanofluid could flow through the tiny passage in MEMS to improve the efficiency. In the

transportation industry, nanocars, General Motors (GM), Ford among others are focusing on nanofluid research projects. Some common applications are:-

- Engine cooling and transmission oil
- Boiler exhaust flue gas recovery
- Cooling of electronic circuits
- Nuclear system cooling
- Solar water heating
- Refrigeration (domestic and chillers)
- Defence and Space applications
- Thermal storage
- Bio-medical applications
- Drilling and lubrications

The measurement of nanofluid critical heat flux (CHF) in a forced convection loop is useful for the nuclear applications. If nanofluid improves the chiller efficiency by 1%, a saving of 320 billion KWh of electricity or equivalent 5.5 million barrel of oil per year would be released in US alone. The nanofluids find the potential for deep drilling operations. A nanofluid can also be used for increasing the dielectric strength and life of transformer oil by dispersing nanodiamonds particles.

1.6 Nanoparticles Solid Volume Fraction

The nanoparticles solid volume fraction is defined as ϕ which is divided by the volume of all constituents of the nanofluid. The volume fraction coincides with the volume concentration in ideal solutions where the volumes of the constituents are additive (the volume of the solution is equal to the sum of the volumes of its ingredients).

The sum of all volume fractions of a mixture is equal to 1:

$$\sum_{i=1}^N \phi_i = 1$$

1.7 Channel Flow

Channel flow constitutes a very important class of flows in fluid dynamics due to its several applications in biological and engineering systems. Therefore, it is necessary to study the characteristics of this flow. In the late 19th century, Maurice Marie Alfred Couette (professor of physics, University of Angers) discovered the laminar flow of a viscous fluid in the space between two parallel plates, one of which is moving relative to other. The flow is driven by virtue of drag force acting on the fluid and applied pressure gradient parallel to the plates is called Couette flow. J.L.M. Poiseuille (1893) studied steady viscous fluid flow between two parallel stationary plates due to an imposed constant pressure gradient generally known as Poiseuille flow. Jeffery (1915) and Hamel (1916), which called classical Jeffery-Hamel flow through convergent-divergent channel, first analyzed the flow between two plates that meet at an angle. Various applications of this type of mathematical models are necessary to understand the flow of rivers and canals, enhancing heat transfer of heat exchangers for milk flow, cold drawing operation in polymer industry, extrusion of molten polymers through converging dies and blood flow of human body. The theoretical study of MHD channel has been a subject of great interest due to its extensive applications in designing cooling system with liquid metals, MHD generators, accelerators, pumps and flow meters (Cha et al. (2002), Tender (1983)).

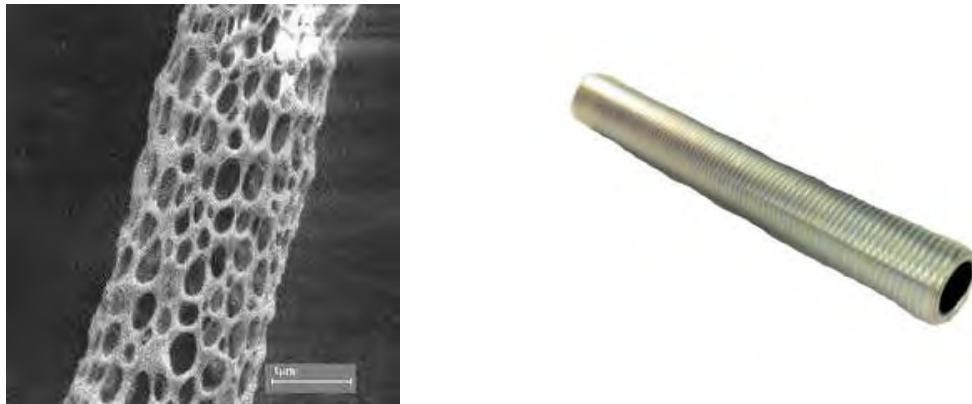


Figure 1.3: Porous Channel

1.8 Power series

Consider a function $U(x)$ which can be represented by a *power series*

$$U(x) = \sum_{i=0}^{\infty} a_i x^i \quad \text{as } x \rightarrow 0 \quad (1.8.1)$$

Let us suppose the N^{th} partial sum is

$$U_N(x) = \sum_{i=0}^{N-1} a_i x^i \quad (1.8.2)$$

the series said to be convergent if the sequence of partial sums converges. When the series converges, the sum $U(x)$ can be approximated by the partial sum $U_N(x)$ and the error can be defined by

$$e_N(x) = U(x) - U_N(x), \quad (1.8.3)$$

The absolute error is defined by

$$e'_N(x) = \left| \frac{e_N(x)}{U(x)} \right|, \quad \text{provided } U(x) \neq 0 \quad (1.8.4)$$

The number of accurate decimals for some particular value of x is given by

$$\rho_N = -\log_{10} |e_N| \quad (1.8.5)$$

It is said that the error decays exponentially if there exists a positive constant \mathcal{E} such that

$\mathcal{E}_N \rightarrow \mathcal{E}$ as $N \rightarrow \infty$, where

$$\mathcal{E}_N = -\frac{\ln |e_N|}{N} \quad (1.8.6)$$

It is also said that the error decays super exponentially if there exists a positive constant ζ such that

$\zeta_N \rightarrow \zeta$ as $N \rightarrow \infty$, where

$$\zeta_N = -\frac{\ln |e_N|}{N \ln N} \quad (1.8.7)$$

An important characteristic of a series is its domain of convergence. If the series $U(x)$ converges for some x_c it also converges absolutely in the open disc

$$\{x: x < |x_c|\}$$

with centre at origin.

1.9 Singularity analysis

Singularities are the important points of a function, because the expansion of a function into a power series depends on the nature of singularities of function. Several types of singularities may arise in physical problems. We are interested to analyze those functions, which have several types of singularities. Practically, one of these singularities dominates the function. Therefore, it is important to know about this singular point to analyze the critical behavior of the function around this point.

The convergence of the sequence of partial sums depends crucially on the singularities of the function represented by the series. The dominating behavior of the function $u(x)$ is represented by a series may be written as

$$u(x) \sim A \left(1 - \frac{x}{x_c}\right)^\alpha \text{ as } x \rightarrow x_c \quad (1.9.1)$$

Where A is constant and x_c is the critical point with the critical exponent α . If α is a negative integer then the singularity is pole, otherwise if it is a nonnegative rational number then the singularity point is branch point. We can include the correction terms with the dominating part in (1.9.1) to estimate the degree of accuracy of the critical points. It can be as follows

$$u(x) \sim A \left(1 - \frac{x}{x_c}\right)^\alpha \left[1 + A_1 \left(1 - \frac{x}{x_c}\right)^{a_1} + A_2 \left(1 - \frac{x}{x_c}\right)^{a_2} + \dots \right] \text{ as } x \rightarrow x_c \quad (1.9.2)$$

Where $0 < a_1 < a_2 < M$ and A_1, A_2, M are constants for some $a_i + \alpha \notin \mathbb{N}$, then the correction terms are called confluent. Sometimes the correction terms can be logarithm e.g.

$$u(x) \sim A \left(1 - \frac{x}{x_c}\right)^\alpha \left[1 + \ln \left| 1 - \frac{x}{x_c} \right| \right] \text{ as } x \rightarrow x_c \quad (1.9.3)$$

Sometimes the sign of the series coefficient indicates the location of the singularity. If the terms are same, the sign of the dominant singular point lies on the positive x-axis. If the terms take alternately positive or negative signs then the singular point is on the negative x-axis. Following are few examples with different type of singularities:

Example:-

1. Singularities that are pole:

$$u(x) = (1-x)^{-3} + \cos(2x).$$

Where $u(x)$ is an algebraic function whose singularity at $x_c = 1$, the critical exponent $\alpha = -3$, which makes the singularity a pole.

2. Algebraic singularities with different exponents:

$$u(x) = (2-x)^{-\frac{1}{2}} + \left(1-\frac{x}{4}\right)^{-\frac{1}{3}} + \left(1-\frac{x}{3}\right)^{-\frac{1}{4}}.$$

Here $u(x)$ have several singular points. The singular points are at $x_c = 2, 4, 3$ and the critical exponents are $\alpha = -\frac{1}{2}, -\frac{1}{3}, -\frac{1}{4}$ respectively. In this example the singular points are branch points. Though there are a number of singularities for $u(x)$, only one of these singularities will dominate the local behavior of $u(x)$.

3. Logarithmic singularity:

$$u(x) = \ln\left(1+\frac{x}{7}\right) + \sin(x).$$

Here $u(x)$ has logarithmic singularity at $x_c = -7$.

4. Exponential singularity:

$$u(x) = \exp(1-4x)^{-3}.$$

Here $u(x)$ has exponential singularity at $x_c = \frac{1}{4}$ with critical exponent $\alpha = -3$.

5. Algebraic dominant singularity with a secondary logarithm behavior:

$$u(x) = \left(1-\frac{x}{3}\right)^{-\frac{1}{2}} + \ln\left(1-\frac{x}{5}\right).$$

The algebraic dominant singularity of $u(x)$ here is at $x_c = 3$ with critical exponent $\alpha = -\frac{1}{2}$ which makes it a branch point and a logarithmic singularity at $x_c = 5$.

6. Nth root singularity:

$$u(x) = \left(1 - \frac{x}{5}\right)^{\frac{1}{n}} + \exp(3x).$$

Here $u(x)$ has a branch point with the critical exponent $\alpha = -\frac{1}{n}$ at $x_c = 5$.

1.10 Elementary bifurcation Theory

A bifurcation occurs where the solution of nonlinear systems alters their qualitative behavior while a parameter changes its value. Particular bifurcation theory shows how the number of steady solutions of a system depends on parameters. Examples of bifurcation are simple turning points in which the number of real solutions become complex conjugate solutions and pitchfork bifurcation in which the numbers of real solutions change discontinuously from one to three (vice versa). We intend to introduce some basic concepts of bifurcation theory. Drazin (1996) discussed the bifurcation theory in detail.

Consider a function map $F: \mathcal{R} \rightarrow \mathcal{R}$. We seek for the solutions

$$u = u(x) \text{ of } F(x, u) = 0 \tag{1.10.1}$$

Bifurcation diagrams can show the solutions. In these diagram solution curves are drawn in the (x, u) plane. Let (x_0, u_0) be a solution of (1.10.1) i.e.

$$F(x_0, u_0) = 0 \tag{1.10.2}$$

Then F can be expanded in Taylor's series about (x_0, u_0) and we can study the solution set in that neighborhood provided that F is smooth. Thus we obtain

$$0 = F(x, u) = F(x_0, u_0) + (u - u_0)F_u(x_0, u_0) + (x - x_0)F_x(x_0, u_0) + \frac{1}{2}(u - u_0)F_{uu}(x_0, u_0) + \dots \tag{1.10.3}$$

If we assume that $F_u(x_0, u_0) = 0$, then

$$U(x) = u_0 - (x - x_0) \frac{F_x(x_0, u_0)}{F_x(x_0, u_0)} + O(x - x_0) \text{ as } x \rightarrow x_0. \tag{1.10.4}$$

This gives only one solution curve in the neighborhood of the point (x_0, u_0) in the bifurcation diagram. However if we replace (x_0, u_0) with (x_c, u_c) where

$$F(x_c, u_c) = 0 \quad (1.10.5)$$

Then the expression (1.10.5) shows that there are at least two curves in the neighborhood of (x_c, u_c) . The point (x_c, u_c) is called bifurcation point.

1.11 Literature review

Nanofluid is a new dynamic subclass of nanotechnology-based heat transfer fluids obtained by dispersing and stably suspended nanoparticles with typical dimensions of shape and size 1-100nm Choi (2007). MHD Nanofluid flows through porous medium has received attention of many researchers due to its applications in technological and engineering problems such as MHD generator; plasma studies, nuclear reactors, geothermal energy extraction. Zubair et al. (2016) studied heat and mass transfer analysis in a viscous unsteady MHD nanofluid flow through a channel with porous walls and medium in the presence of metallic nanoparticles. R.Elahi et al. (2014) studied theoretical study of blood flow of nanofluid through composite stenosed arteries with permeable walls. The problem of laminar nanofluid flow in a semi-porous channel in the presence of transverse magnetic field was investigated analytically by Sheikholeslami et al. (2014). M. Sheikholeslami and D.D. Ganji (2013) studied Heat transfer of Cu-water nanofluid flow between parallel plates. M. Sheikholeslami et al.(2014) studied Nanofluid flow and heat transfer in a rotating system in the presence of magnetic field. Their results showed that velocity boundary layer thickness decreases with the increase of Reynolds number and it increases as Hartmann number increases.

Majdalani et al. (2002) studied two dimensional viscous flows between slowly expanding, contracting walls with weak permeability. H.N. Chang et al (1989) studied velocity field of pulsatile flow in a porous tube. Their result found that Seepage across permeable walls is clearly important to the mass transfer between blood, air and tissue. Therefore, a substantial amount of research work has been invested in the study of the flow in rectangular domain bounded by two moving porous walls, which enable the fluid to enter or exit during successive expansions or contractions. Dauenhauer et al. (1999) studied the unsteady flow in semi-infinite expanding

channels with wall injection. They are characterized by two non-dimensional parameters, the expansion ratio of the wall α and the cross-flow Reynolds number Re . Hatami et al.(2015) studied numerical analysis of nanofluid flow conveying nanoparticles through expanding and contracting gaps between permeable walls. Boutros et al (2006) studied the solution of the Navier-stokes equations which described the unsteady incompressible laminar flow in semi-infinite porous circular pipe with injection or suction. Through the pipe wall whose radius varies with time. The resulting fourth-order nonlinear differential equation is then solved using small parameters perturbations. Majdalani and Zuhu (2003) studied moderate to injection and suction driven channel flow with expanding and contracting channel. Using perturbations in cross-flow Reynolds number Re , the resulting equation is solved both numerically and analytically. Zaimi et al. (2014) discussed the unsteady flow, heat and mass transfer analysis for nanofluids through a contracting cylinder. Fakour et al. (2015) showed an analytical solution for micropolar fluid flow through a channel with porous walls. Jashim et al. (2012) demonstrated the mathematical modeling of MHD thermosolute nanofluid flow in porous medium under the influence of convection slip conditions. Hayat et al. (2009) presented an analysis of heat transfer on the peristaltic flow with porous medium. Sacheti (2003) discussed the Brinkman model for the steady poiseulle flow of a viscous incompressible fluid in a porous channel. Various researchers have all that much purposeful this idea and the points of interest can be found in writing. Hatami et al. (2003) discussed the laminar nanofluid flow in a semi-porous channel with magnetic field effect through using porous fins. Kashif et al. (2014) considered the heat and mass transfer flow with the impact of penetrable Reynolds number and relaxing/contracting parameter in the vicinity of metallic-oxide nanoparticles between orthogonally moving permeable disks. Zaimi et al. (2014) discussed the unsteady flow, heat and mass transfer analysis for nanofluids through a contracting cylinder. By using the two-phase model of nanofluid flow, heat and mass transfer in a rotating system in the presence of a magnetic field was investigated by Sheikholeslami et al.(2014). The flow and heat transfer in porous tube or channel has been studied by a number of authors (Wernert et al. (2005), Jafari et al. (2009), Georke (2002)).Berman (1953) described an exact solution of the Navier-Stokes equation for steady two-dimensional laminar flow of a viscous, incompressible fluid in a channel with parallel rigid porous walls driven by uniform suction or injection at the walls. Finally, Hatami et al (2013) studied Analytical investigation of MHD nanofluid in Semi porous channel.

In discussion unsteady magnetohydrodynamics (MHD) nanofluid flow through expanding and contracting channel flow with permeable walls are studied. The reduced non-dimensional fourth order differential equation solved by Hermite- Padé approximation method. Then result displayed graphically.

1.12 Objectives of this thesis:

A review of earlier studies indicates that none has used MHD in such a channel. The present study investigates the stability of the magnetohydrodynamics flow through the channel. The aim is to represent model geometrically and formulate mathematically using governing equations and boundary conditions. Then the equations are making dimensionless by using suitable transformations. A polynomial series will be determined from the dimensionless equation and then analyzed by using approximation method with the help of algebraic programming language. The target is to determine the dominating singularity behavior of the problem and to compare the result with others. The results will be displayed graphically. The specific objectives of the present research work are:

- To reproduce Hatami et al. (2015) result by using approximation method.
- To find bifurcation point using governing equations and boundary conditions.
- To analyze singularity behavior of the problem numerically and graphically.
- To investigate the effect of governing parameters namely, Reynolds number Re , Hartmann number Ha , non-dimensional wall dilation rate α , nanoparticle solid volume fraction ϕ .
- To compare the result of the present investigation with similar published work.

It is expected that the present numerical and graphical investigation will contribute to search more efficient finding and to make new dimension in research area.

1.13 Organization of Thesis

In chapter 1, a brief introduction is presented with significance and objective of the study. This chapter consists of physical phenomena of fluid, Magneto hydrodynamics (MHD), Nanofluid, Nanoparticle solid volume fraction, channel flow with applications. Also consists of power series, singularity analysis and elementary bifurcation theory with example. A literature review of the past studies on the above physical facts is included.

In chapter 2, the numerical procedures for solving nonlinear dimensionless equations are discussed.

In chapter 3, the basic governing equation for the flow fields are shown in standard vector form and mathematical modeling of the problem for various case is discussed.

Magnetohydrodynamics (MHD) nanofluid flow through expanding and contracting channel flow with permeable walls are studied in chapter 4. The influence of the governing flow parameters namely Reynolds number, Hartmann number, non-dimensional wall dilation rate, nanoparticle solid volume fraction on stream function and velocity profile are shown. Shear stress is presented for different values of above parameters. Moreover, bifurcation point is found.

A summary of major conclusions and some schemes of further work are expressed in Chapter 5.

Approximation Methods

The numerical procedures as approximation method for solving nonlinear dimensionless governing equations of the problem is in this chapter.

2.1 Introduction

This thesis is concerned with the techniques for summing power series that can be described collectively as approximation method to reveal the local behavior of series around its singular point and the critical relationship among the solution parameters.

The approximation methods are widely used to approximate functions in many areas of applied mathematics. A function is said to be approximant for a given series if its Taylor series expansion reproduces the first terms of the series.

Padé (1892) and Hermite (1893) introduced a very efficient solution method, known as Hermite-Padé approximants. Blanch(1964) evaluated continued function fractions numerically. Brezinski(1990) studied history of continued fraction and approximants. Also, application of continued fractions and their generalizations of problems in approximation theory have been studied by khovanskii (1963). Baker and Graves-Moris (1996) studied Padé approximants and its properties. Algebraic and Differential approximants (1978) are some useful generalizations of Padé approximants and its properties. Khan (2001) analyzed singularity behavior by summing power series. Khan (2002) also introduced a new model of differential approximant for single independent variable for the summation of power series called High-order differential approximant (HODA). The method is special type of Hermite- Padé class and it is one of the best methods of singularity analysis for the problems of single independent variable. High-order partial differential approximants discussed in Rahman (2004) is a multivariable differential approximants.

2.2 Hermite- Padé approximants

The entire one variable approximants that are used or discussed throughout this thesis paper belongs to the Hermite- Padé class. In its most general form, this class is concerned with the

simultaneous approximation of several independent series and there are some advantages in first describing the Hermite- Padé class from that point of view.

Let $d \in \mathbb{N}$ and the $d+1$ power series

$$U_0(x), U_1(x), \dots, U_d(x)$$

are given. We say that the $(d+1)$ – tuple of polynomials

$$\{P_N^{[0]}, P_N^{[1]}, \dots, P_N^{[d]}\},$$

where

$$\deg P_N^{[0]} + \deg P_N^{[1]} + \dots + \deg P_N^{[d]} + d = N, \quad (2.2.1)$$

is a Hermite- Padé form of these series if

$$\sum_{i=0}^d p_N^{[i]}(x) U_i(x) = O(x^N) \quad \text{as } x \rightarrow 0 \quad (2.2.2)$$

Here $U_0(x), U_1(x), \dots, U_d(x)$ may be independent series or different form of a unique series.

We need to find $P_N^{[i]}$ that satisfy the equations (2.2.1) and (2.2.2). These polynomials are completely determined by the coefficients. So, the total number of unknowns in equation (2.2.2) is

$$\sum_{i=0}^d \deg P_N^{[i]} + d + 1 = N + 1 \quad (2.2.3)$$

Expanding the left hand side of the equation (2.2.2) in powers of x , it is found that the equation (2.2.2) is equivalent to equating the first N terms in the expansion to zero. We get a system of N linear homogenous equations for the unknown coefficients of the polynomials. To calculate the coefficients of the Hermite- Padé polynomials we require some sort of normalization, such as

$$P_N^{[i]}(0) = 1 \quad \text{for some } 0 \leq i \leq d. \quad (2.2.4)$$

The equation (2.2.3) simply ensures that the coefficient matrix associated with the system is square. One way to construct the Hermite- Padé polynomial is to solve the system of linear equations by any standard method such as Gaussian elimination or Gauss-Jordan elimination. The computed complexity of this approach is

$O(N^{\beta})$ (work), $O(N^2)$ (storage) as $N \rightarrow \infty$.

It is important to emphasize that the only input required for the calculation of the Hermite- Padé polynomials are the first N coefficients of the series U_0, U_1, \dots, U_d .

2.3 Padé Approximants

Padé approximant is a technique for summing power series that is widely used in applied mathematics as Van Dyke (1975). In the Padé method, the approximant is sought in the class of rational functions. Padé approximants can be described from the Hermite- Padé class in the following sense.

In the Hermite- Padé class, let $d=1$ and the polynomials $P_N^{[0]}$ and $P_N^{[1]}$ satisfy equations (2.2.1) and (2.2.2). One can define an approximant $u_N(x)$ of the series $U(x)$ by

$$P_N^{[1]}u_N - P_N^{[0]} = 0, \tag{2.3.1}$$

Where, $U_1 = U$ and $U_0 = -1$

Then we select the polynomials

$$P_N^{[0]}(x) = \sum_{i=0}^n b_i x^i \text{ and } P_N^{[1]}(x) = \sum_{i=0}^m c_i x^i \tag{2.3.2}$$

Such that $(n + m) \leq N$, the constants b_i 's and c_i 's are unknown to be determined. So that,

$$u_N(x)P_N^{[1]}(x) - P_N^{[0]}(x) = O(x^{n+m+1}) \tag{2.3.3}$$

Equating the first $(n + m)$ equations of (2.3.3) equal to zero and the normalization condition in equation (3.2.4), we find the values of b_i 's and c_i 's. Then, the rational approximant is known as

Padé approximant denoted as

$$u_N(x) = \frac{P_N^{[0]}(x)}{P_N^{[1]}(x)}, \tag{2.3.4}$$

Padé approximant has often been used to obtain information about the singularity structure of a function from its series coefficients. The main idea to examine the behavior of the denominators $P_N^{[1]}$. The Padé approximants is also have been used is tacking slowly convergent, divergent and asymptotic series. The zeroes of the denominator $P_N^{[1]}$ give the singular point such

as pole of the function $u(x)$ if it exists. If a sequence of zeros approaches a limit as N increases, then the limit is almost certainly a singularity of $U(x)$. In order to evaluate the Padé approximants for a given series numerically, we have used symbolic computation language such as MAPLE.

Examples 2.1: consider $u(x) = \frac{1}{(1-x)^2} + e^{2x}$, a function with a simple pole. After applying the normalization condition $c_0=1$, we obtain the polynomial coefficients $P_5^{[0]}$ and $P_5^{[1]}$ for $\deg P_5^{[0]}=n$ and $\deg P_5^{[1]}=m$ when $m=n=2$,

$$P_5^{[0]} = 1 - \frac{175}{61}x + \frac{181}{122}x^2 \quad \text{and}$$

$$P_5^{[1]} = -\frac{345}{122} + \frac{268}{81}x - \frac{321}{122}x^2.$$

When $m=n=3$,

$$P_7^{[0]} = 1 - \frac{287}{27}x + \frac{1}{2}x^2 + \frac{47}{27}x^3$$

And $P_7^{[1]} = -\frac{385}{54} + \frac{85}{9}x - \frac{125}{54}x^2 + \frac{8}{81}x^3.$

The table below will show the convergence to the singular point of Padé approximant.

Table 2.1: The approximant of x_c by Padé for the function in example 2.1

m, n	x_c
2,2	.1899603214 + .1471159877i
3,3	2.609057312 - .1 × 10 ⁻⁸ i

2.4 Algebraic approximants

Algebraic approximant is a special type of Hermite- Padé approximants. In the Hermite- Padé class, we take

$$d \geq 1, U_0 = 1, U_1 = U, \dots, U_d = U^d. \quad (2.4.1)$$

An algebraic approximant $u_N(x)$ of the series $U(x)$ can be defined as solution of the equation (2.4.1) is a polynomial of the partial sum $u_N(x)$ in degree d , the algebraic approximants $u_N(x)$, is in general a multivalued function with d branches. At first this may appear to be an undesirable feature of the method, in that case we have the problem of identifying the particular branch that approximates $U(x)$. On the other hand, the series $U(x)$ is the expansion of the particular type of function $u(x)$ that is itself multivalued. For Algebraic approximants, one uses the partial sum $u_N(x)$ to construct the $(d+1)$ polynomials

$$\{P_N^{[0]}(x), P_N^{[1]}(x), \dots, P_N^{[d]}(x)\},$$

Such that

$$\sum_{i=0}^d p_N^{[i]}(x) u_N^i(x) = O(x^N) \quad (2.4.2)$$

And
$$\sum_{i=0}^d \deg P_N^{[i]} + d = N, \quad (2.4.3)$$

The total number of unknown in the equations (2.4.2) is

$$\sum_{i=0}^d \deg P_N^{[i]} + d + 1 = N + 1 \quad (2.4.4)$$

In the order of determine the polynomial the coefficient of the polynomials $P_N^{[i]}$ one can set $P_N^{[0]}(0) = 1$ for normalization, without loss of generality. The discriminant of the equation (2.4.1) approximates the singularity of function $u(x)$.

Example 2.2: consider $u(x) = (1+3x)^{\frac{1}{3}} + \sin(2x)$.

Let $d=2$ and $\deg P_8^{[0]} = \deg P_8^{[1]} = \deg P_8^{[2]} = 2$ to apply the algebraic approximation method on the power series of the function. After we set the normalization condition $P_8^0 = 1$ we get the polynomials

$$P_8^{[0]}(x) = 1 - \frac{10246192803431}{2514550532711}x - \frac{744734102789}{2514550532711}x^2$$

$$P_8^{[1]}(x) = \frac{3180134571291}{12572752663555} - \frac{5416308772923}{12572752663555}x + \frac{828242251983}{2514550532711}x^2$$

$$P_8^{[2]}(x) = \frac{5765716034292}{12572752663555} - \frac{60179793102}{12572752663555}x - \frac{50166000897}{12572752663555}x^2$$

Here the discriminant gives us the singularity at $x_c = .2093493364$. If we increase the degree of the polynomial coefficients, it may give us a better approximation. So again

Let $d=2$ and $\deg P_8^{[0]} = \deg P_8^{[1]} = \deg P_8^{[2]} = 3$, following the same process we get this singularity is calculated at $x_c = .1848860209$.

Again taking $d=2$ and $\deg P_8^{[0]} = \deg P_8^{[1]} = \deg P_8^{[2]} = 4$ the singularity is calculated at $x_c = -0.01002326757$. The table below will show the comparative results of the convergence of the algebraic method to the singular point.

Table 2.2: the approximation of x_c by algebraic approximant for the function in upper example.

$\deg P_N^{[i]}$	d	x_c
2	2	0.2093493364
3	2	0.1848860209
4	2	-0.01002326757

Note that $d=3$ may be more accurate for this problem.

2.5 Drazin-Tourigney Approximants

Drazin and Tourigney in (1996) implemented the idea that $d=O(\sqrt{N})$ as $N \rightarrow \infty$. Their method is simply a particular kind of algebraic method, satisfying the equations

$$P_N^{[0]}(x) + P_N^{[1]}(x)u_N(x) + P_N^{[2]}(x)u_N^2(x) + \dots + P_N^{[d]}(x)u_N^d(x) = 0 \quad (2.5.1)$$

In this method they considered

$$\deg P_N^{[i]} = d - i \quad (2.5.2)$$

And $N = \frac{1}{2}(d^2 + 3d - 2)$. (2.5.3)

There is a recurrence relation for the calculation of the Drazin-Tourigney polynomial, but its order increases with N . At present, nothing is known about the convergence of this approximants. However, Drazin and Tourigney (2000) present some numerical results that suggest that the error for this series of (3.5.1) decays super exponentially.

Drazin and Tourigney initially motivated in (1996) to solve boundary value problems for nonlinear systems of ordinary and partial differential equations.

2.6 Differential Approximants

Differential approximants is an important member of Hermite- Padé class. It is obtained by taking

$$d \geq 2, U_0 = 1, U_1 = U, U_2 = DU, \dots, U_d = D^{d-1}U. \quad (2.6.1)$$

Where $D \equiv \frac{d}{dx}$ is the differential operator, the differential approximants $u_N(x)$ of the series $U(x)$ can be defined as the solution of the differential equation

$$P_N^{[0]} + P_N^{[1]}u_N + P_N^{[2]}Du_N + \dots + P_N^{[d]}D^{d-1}u_N = 0 \quad (2.6.2)$$

A popular variant is obtained by taking

$$d \geq 1, U_0 = 1, U_1 = DU, U_2 = D^2U, \dots, U_d = D^dU. \quad (2.6.3)$$

Instead of (2.6.1). This gives the homogenous linear differential equation

$$P_N^{[0]}u_N + P_N^{[1]}Du_N + P_N^{[2]}D^2u_N + \dots + P_N^{[d]}D^d u_N = 0 \quad (2.6.4)$$

For the approximants.

Here (2.6.2) is a linear differential equation of order (d-1) with polynomial coefficients. There are (d-1) linearly independent solutions, but only one of them has the same first few Taylor coefficients as the given series $U(x)$. When $d > 2$, the usual method for solving such an equation is to construct a series solution.

Differential approximants are chiefly for series analysis. They are powerful tools for locating singularities of a series and for identifying their nature. In this respect, the key is to note that it is not necessary to solve the differential equation (2.6.2) in order to find the singularities of $u_N(x)$. The only singularities of $U(x)$ are located at the zeroes of the leading polynomial $P_N^{d-1}(x)$. Hence, some of the zeroes of $P_N^{d-1}(x)$ may provide approximations of the singularities of the series $U(x)$. For instance, if $u_N(x)$ has a singularity at $\lambda = \lambda_{\epsilon, N}$ of the algebraic type

$$u_N \sim u_{0, N} + u_{1, N}(\lambda - \lambda_{\epsilon, N})^{\alpha_N},$$

Then the exponents α_N is given by the simple formula

$$\alpha_N = d - 2 - \frac{P_N^{d-1}(\lambda_{\epsilon, N})}{D P_N^d(\lambda_{\epsilon, N})}.$$

Example 2.3 Consider $u(x) = \frac{e^x(1+\sin(x))}{\sqrt{1-\frac{1}{3}x}}$.

Taking $d=3$ for $\sum_{i=0}^d \deg P_N^{[i]} + d = N$ and applying $\deg P_N^{[0]} + \deg P_N^{[1]} + \dots + \deg P_N^{[d]} + d = N$,

and $\sum_{i=0}^d p_N^{[i]}(x)U_i(x) = O(x^N)$, we obtain the singular point at $x_c = 2.991301923$. In similar procedure taking $d=4$ gives us more accurate result, i.e. $x_c = 2.999999734$. The table below shows a comparative result.

Table 2.3: The approximation of x_c by Differential approximant for the above function.

N	d	x_c
15	2	3.000563091
21	3	2.991301923
28	4	2.999999734

2.7 High Order Differential Approximants (HODA)

Khan (2002) introduced an extension of differential approximant, which he mentioned as High order differential approximant. When the function has a countable infinity of branches, then the fixed low-order differential approximant may not be useful. So, for these cases he considers d increase with N . It leads to a particular kind of differential approximant $u_N(x)$, satisfying (2.6.2), i.e.

$$P_N^{[0]} + P_N^{[1]}u_N + P_N^{[2]}Du_N + \dots + P_N^{[d]}D^{d-1}u_N = 0$$

Where

$$N = \frac{1}{2}d(d+3) \tag{2.7.1}$$

And

$$\deg P_N^{[i]} = i \tag{2.7.2}$$

From (2.7.2) he deduced that there are

$$\sum_{i=0}^d (i+1) = \sum_{i=0}^{d+1} i = \frac{1}{2}(d+1)(d+2)$$

Unknown parameters in the definition of the Hermite- Padé form. In order to determine those parameters, the N equation used that follow from (2.2.2)

$$P_N^{[0]}(x) + \sum_{i=1}^d P_N^{[i]}(x)D^i U(x) = O(x^N) \text{ as } x \rightarrow 0.$$

In addition, one can normalize by setting $P_N^{[d]}(0)=1$. Then there remain as many equations as unknowns. One of the roots, say $\lambda_{c,N}$, of the coefficient of the highest derivative, i.e.

$$P_N^{[d]}(\lambda_{c,N})=0.$$

gives an approximation of the dominant singularity λ_c of the series U . If the singularity is of algebraic type, then the exponent may α be approximated by

$$\alpha_N = d - 2 - \frac{P_N^{(d-1)}(\lambda_{c,N})}{DP_N^{(d)}(\lambda_{c,N})}. \tag{2.7.3}$$

It is worth noting that the formulae for the location and the exponent of the dominant singularity involve only the coefficients of the highest derivatives in the differential equation that defines the approximant. This motivates the choice (2.7.2) with its emphasis on those very coefficients.

2.8 High-Order Partial Differential Approximants (HPDA)

Consider the function $f(x,y)$ of two independent variables, represented by its power series

$$U(x,y) = \sum_{i=0}^{\infty} \sum_{j=0}^{\infty} c_{ij} x^i y^j \quad \text{as } (x,y) \rightarrow (0,0) \tag{2.8.1}$$

And the partial sum

$$U_N(x,y) = \sum_{i=0}^{N-1} \sum_{j=0}^{N-1} c_{ij} x^i y^j \tag{2.8.2}$$

By using that partial sum, the following $(2d+1)$ polynomials can be constructed

$$P_{[0,0]}, P_{[1,0]}, P_{[0,1]}, \dots, P_{[d,0]}, P_{[0,d]} \tag{2.8.3}$$

In x and y such that

$$P_{[0,0]}U_N + P_{[1,0]}\frac{\partial U_N}{\partial x} + P_{[0,1]}\frac{\partial U_N}{\partial y} + \dots + P_{[d,0]}\frac{\partial^d U_N}{\partial x^d} + P_{[0,d]}\frac{\partial^d U_N}{\partial y^d} = \sum_{i=0}^{\infty} \sum_{j=0}^{\infty} c_{ij} x^i y^j \tag{2.8.4}$$

Where $e_j = 0$ for $i+j < N=3d-1$ (2.8.5)

By equating the coefficients of the variables and their powers from (2.8.5), one can obtain a total of

$$N_e = \frac{1}{2} 3d(3d-1) \quad (2.8.6)$$

Equations to determine the unknown coefficients of the polynomials in (2.8.3), the normalization condition can be imposed

$$P_{[0,0]}=1 \quad \text{or} \quad P_{[d,0]}=1 \quad \text{or} \quad P_{[0,d]}=1 \quad \text{for} \quad (x,y) \rightarrow (0,0) . \quad (2.8.7)$$

Thus, remaining unknowns

$$N_u = \frac{1}{3} d(d^2 + 6d + 11) \quad (2.8.8)$$

must be found by the use of N_e equations.

It would be helpful to write the system of linear equations $e_{i,j} = 0$ into the matrix form with the $N_e \times 1$ unknown matrix \underline{x} .

Thus, the non-homogenous system of N_e linear equations with N_u unknowns can be written in matrix form as

$$\underline{A}\underline{x} = \underline{b} \quad (2.8.9)$$

Where A is $N_e \times N_u$ matrix and \underline{b} is the non-zero column matrix of order $N_e \times 1$. Thus, system will be solvable if

$$N_e \leq N_u \quad (2.8.10)$$

However, the system may be inconsistent. If the system is consistent, then the system can be solved by converting the augmented matrix $[A/\underline{b}]$ to row echelon or reduced row echelon form by using the Gaussian elimination or Gauss-Jordan elimination. It is noted that, there will exist some free variables. Naturally the values of the free variables in the multivariable approximant methods can be chosen at random. There is no particular reason to pick up these particular numbers. It might for instance seek a solution such that the polynomials in (2.8.3) have as few high-order terms as possible. Usually the accuracy of the method does not depend critically on the particular choice made. Once the polynomials (2.8.3) have been found, it is more practical to find the singular points by solving either of the polynomial coefficients of the highest derivatives $P_{[d,0]}(x,y) = 0$ or $P_{[0,d]}(x,y) = 0$ or both simultaneously.

Governing Equations of the Problem

The basic governing equations for the flow in standard vector form and the mathematical modeling of the problem for various cases with different coordinate systems are represented in this chapter.

3.1: Introduction

The basis of computational fluid dynamics is the basic fluid dynamical governing equations; the continuity, the momentum (Navier-Stokes equation) and the energy equations. These equations depict the physics of various flows. They are the mathematical statements of the three fundamental laws or principles upon which fluid dynamics is based:

- Mass is conserved for a system;
- Second law of Newton;
- First law of Thermodynamics; Energy is conserved.

3.2: Continuity Equation

The continuity equation is based on the mass conservation principle, which states that mass can neither be created nor be destroyed. Conservation of mass is inherent to a control mass system (closed system). The above law is stated mathematically as:

$$\frac{\Delta m}{\Delta t} = 0 \quad (3.2.1)$$

Where m = mass of the system.

The equation of continuity in vector form is written as

$$\frac{\partial \rho}{\partial t} + \nabla \cdot (\rho \underline{q}) = 0, \quad (3.2.2)$$

Where $\underline{q} = u\hat{i} + v\hat{j} + w\hat{k}$ is the velocity of flow at a point and ρ the density of the fluid.

For a steady flow $\frac{\partial \rho}{\partial t} = 0$, thus

$$\nabla \cdot (\rho \underline{q}) = 0, \quad (3.2.3)$$

For incompressible fluid flow, $\rho = \text{constant}$, hence the continuity equation becomes

$$\nabla \cdot \underline{q} = 0. \quad (3.2.4)$$

3.3 Momentum Equation (Navier-Stokes Equation)

This equation is formed by applying another fundamental physical principle to a model of the flow, namely Physical principle. Newton's second law on the moving fluid element, states that the net force on the fluid equals its mass times the acceleration of the element.

$$\underline{F} = m\underline{a} \quad (3.3.1)$$

The momentum equations are called the Navier-Stokes equations in honour of two men-the Frenchman M. Navier and the Englishmen G. Stokes, who independently obtained the equations in the first half of the nineteenth century.

The Navier-Stokes equations for viscous incompressible fluid with constant viscosity in vector form is expressed as

$$\rho \left(\frac{\partial \underline{q}}{\partial t} + (\underline{q} \cdot \nabla) \underline{q} \right) = \rho \underline{g} - \nabla p + \mu \nabla^2 \underline{q} + \underline{M} \quad (3.3.2)$$

Where \underline{g} denotes the body force per unit mass acting on the fluid element, p is the pressure, μ is the viscosity of the fluid and \underline{M} is the other external force.

3.4 The Governing equations in Cartesian coordinate system

The governing equations (3.2.2) and (3.3.2) in vector form are transformed into the following equations in Cartesian form.

Mass Conservation (continuity) equation

$$\frac{\partial \rho}{\partial t} + \frac{\partial (\rho u)}{\partial x} + \frac{\partial (\rho v)}{\partial y} + \frac{\partial (\rho w)}{\partial z} = 0$$

For incompressible steady fluid flow;

$$\frac{\partial u}{\partial x} + \frac{\partial v}{\partial y} + \frac{\partial w}{\partial z} = 0$$

Momentum (Navier-Stokes) Equations

$$\text{X- direction: } \rho \left(\frac{\partial u}{\partial t} + u \frac{\partial u}{\partial x} + v \frac{\partial u}{\partial y} + w \frac{\partial u}{\partial z} \right) = -\frac{\partial p}{\partial x} + \mu \left(\frac{\partial^2 u}{\partial x^2} + \frac{\partial^2 u}{\partial y^2} + \frac{\partial^2 u}{\partial z^2} \right) + \rho g_x$$

$$\text{Y- direction: } \rho \left(\frac{\partial v}{\partial t} + u \frac{\partial v}{\partial x} + v \frac{\partial v}{\partial y} + w \frac{\partial v}{\partial z} \right) = -\frac{\partial p}{\partial y} + \mu \left(\frac{\partial^2 v}{\partial x^2} + \frac{\partial^2 v}{\partial y^2} + \frac{\partial^2 v}{\partial z^2} \right) + \rho g_y$$

$$\text{Z- direction: } \rho \left(\frac{\partial w}{\partial t} + u \frac{\partial w}{\partial x} + v \frac{\partial w}{\partial y} + w \frac{\partial w}{\partial z} \right) = -\frac{\partial p}{\partial z} + \mu \left(\frac{\partial^2 w}{\partial x^2} + \frac{\partial^2 w}{\partial y^2} + \frac{\partial^2 w}{\partial z^2} \right) + \rho g_z$$

3.5 The Governing equations in Cylindrical coordinate system

The del (∇) operator in cylindrical coordinate system is defined as

$$\nabla \rho = \frac{1}{r} \frac{\partial(\rho r)}{\partial r} + \frac{1}{r} \frac{\partial(\rho)}{\partial \theta} + \frac{\partial(\rho)}{\partial z}$$

The governing equations (3.2.2) and (3.3.2) in vector form are transformed into the following equations in cylindrical coordinate system.

Mass Conservation (continuity) equation

$$\frac{\partial \rho}{\partial t} + \frac{1}{r} \frac{\partial(\rho q_r r)}{\partial r} + \frac{1}{r} \frac{\partial(\rho q_\theta)}{\partial \theta} + \frac{\partial(\rho q_z)}{\partial z} = 0$$

For incompressible steady fluid flow;

$$\frac{\partial q_r}{\partial r} + \frac{q_r}{r} + \frac{1}{r} \frac{\partial q_\theta}{\partial \theta} + \frac{\partial q_z}{\partial z} = 0$$

where q_r , q_θ and q_z be the velocity components in the r , θ , z directions respectively.

Momentum (Navier-Stokes) Equations

$$\rho \left(\frac{\partial q_r}{\partial t} + q_r \frac{\partial q_r}{\partial r} + \frac{q_\theta}{r} \frac{\partial q_r}{\partial \theta} - \frac{q_\theta^2}{r} + q_z \frac{\partial q_r}{\partial z} \right) = -\frac{\partial p}{\partial r} + \mu \left(\frac{\partial^2 q_r}{\partial r^2} + \frac{1}{r} \frac{\partial q_r}{\partial r} - \frac{q_r}{r^2} + \frac{1}{r^2} \frac{\partial^2 q_r}{\partial \theta^2} - \frac{2}{r^2} \frac{\partial q_\theta}{\partial \theta} + \frac{\partial^2 q_r}{\partial z^2} \right) + \rho g_r$$

$$\rho \left(\frac{\partial q_\theta}{\partial t} + q_r \frac{\partial q_\theta}{\partial r} + \frac{q_\theta}{r} \frac{\partial q_\theta}{\partial \theta} + \frac{q_r q_\theta}{r} + q_z \frac{\partial q_\theta}{\partial z} \right) = -\frac{1}{r} \frac{\partial p}{\partial \theta} + \mu \left(\frac{\partial^2 q_\theta}{\partial r^2} + \frac{1}{r} \frac{\partial q_\theta}{\partial r} - \frac{q_\theta}{r^2} + \frac{1}{r^2} \frac{\partial^2 q_\theta}{\partial \theta^2} + \frac{2}{r^2} \frac{\partial q_r}{\partial \theta} + \frac{\partial^2 q_\theta}{\partial z^2} \right) + \rho g_\theta$$

$$\rho \left(\frac{\partial q_z}{\partial t} + q_r \frac{\partial q_z}{\partial r} + \frac{q_\theta}{r} \frac{\partial q_z}{\partial \theta} + q_z \frac{\partial q_z}{\partial z} \right) = \frac{\partial p}{\partial z} + \mu \left(\frac{\partial^2 q_z}{\partial r^2} + \frac{1}{r} \frac{\partial q_z}{\partial r} + \frac{1}{r^2} \frac{\partial^2 q_z}{\partial \theta^2} + \frac{\partial^2 q_z}{\partial z^2} \right) + \rho g_z$$

where g_r , g_θ and g_z be the components body force in the r , θ , z directions respectively.

3.6 Maxwell's Equations

Magnetohydrodynamic equations are the ordinary electromagnetic and hydrodynamic equations modified to take account of the interaction between the motion of the fluid and the electromagnetic field. Formulation of the electromagnetic theory is known as Maxwell's equation. Maxwell's basic equations show the relation of basic field quantities and their construction. Maxwell's equations are:

Charge continuity

$$\nabla \cdot \underline{D} = \rho_e \quad (3.6.1)$$

Current continuity

$$\nabla \cdot \underline{J} = -\frac{\partial \rho_e}{\partial t} \quad (3.6.2)$$

Magnetic field continuity

$$\nabla \cdot \underline{B} = 0 \quad (3.6.3)$$

Ampere's Law

$$\nabla \times \underline{B}_0 = \underline{J} + \frac{\partial \underline{D}}{\partial t} \quad (3.6.4)$$

Faraday's Law

$$\nabla \times \underline{E} = -\frac{\partial \underline{B}}{\partial t} \quad (3.6.5)$$

Constitutive equations for \underline{D} and \underline{B}

$$\underline{D} = \epsilon \underline{E} \quad \text{and} \quad \underline{B} = \mu_e \underline{B}_0 \quad (3.6.6)$$

Total current density flow

$$\underline{J} = \sigma(\underline{E} + \underline{q} \times \underline{B}) + \rho_e \underline{q} \quad (3.6.7)$$

The equations (3.6.1) to (3.6.7) are Maxwell's equation where \underline{D} is the electron displacement, ρ_e is charge density, \underline{E} is the electric field, \underline{B} is the magnetic field, B_0 is the magnetic field intensity, \underline{J} is the current density, $\frac{\partial \underline{D}}{\partial t}$ is the displacement current density, ϵ is the electric permeability of medium, \underline{q} is the velocity vector, σ is the electrical conductivity and $\rho_e \underline{q}$ is the convection current due to charge moving with the field.

In MHD, a fluid is considered as grossly neutral. Then the charge density ρ_e in Maxwell's equation is interpreted as an excess charge density, which is generally not large. If the excess charge density is ignored, then the displacement current is also ignored. In most problems the current due to convection of the excess charge are small. Therefore, the electromagnetic equations can be reduced to the following form:

Charge continuity

$$\nabla \cdot \underline{D} = 0 \quad (3.6.8)$$

Current continuity

$$\nabla \cdot \underline{J} = 0 \quad (3.6.9)$$

Ampere's Law

$$\nabla \times \underline{B}_0 = \underline{J} \quad (3.6.10)$$

Total current density flow

$$\underline{J} = \sigma(\underline{E} + \underline{q} \times \underline{B}) \quad (3.6.11)$$

3.7 General Equations Governing Magnetohydrodynamic Nanofluid flow

3.7.1 The Continuity Equation

The MHD continuity equation for viscous incompressible electrical conductive nanofluid remains as that of usual continuity equation

$$\nabla \cdot \underline{q} = 0. \quad (3.7.1)$$

3.7.2 The Momentum (Navier-Stokes) Equation

The equation of momentum (3.3.2) governing the flow of a nanofluid is expressed as

$$\rho_{nf} \left(\frac{\partial \underline{q}}{\partial t} + (\underline{q} \cdot \nabla) \underline{q} \right) = \rho_{nf} \underline{g} - \nabla p + \mu_{nf} \nabla^2 \underline{q} + \underline{M} \quad (3.7.2)$$

Where \underline{M} is the other external forces acting on the flow.

Taking into account the force due to gravity, thermal expansion and the force per unit volume when an electrical current density \underline{J} flows through the fluid i.e. the Lorentz force $\underline{J} \times \underline{B}$ due to the presence of magnetic field, the Navier-Stokes equation (3.7.2) becomes,

$$\frac{\partial \underline{q}}{\partial t} + (\underline{q} \cdot \nabla) \underline{q} = \frac{1}{\rho_{nf}} [-\nabla p + \mu_{nf} \nabla^2 \underline{q}] + \underline{g} \beta_{nf} \Delta T + \frac{1}{\rho_{nf}} (\underline{J} \times \underline{B}) \quad (3.7.3)$$

Where \underline{q} is the velocity vector, p is the pressure, ρ_{nf} is the density of the nanofluid, μ_{nf} is the dynamic viscosity of the nanofluid and β_{nf} is the thermal expansion coefficient of nanofluid.

Following Sheikholeslami et al.(2012), the relationship between the thermo physical properties of the nanofluid and convectional base fluid together with nanoparticles are given as:

$$\mu_{nf} = \frac{\mu_f}{(1-\phi)^{2.5}}, \quad \rho_{nf} = (1-\phi)\rho_f + \phi\rho_s,$$

$$\frac{\sigma_{nf}}{\sigma_f} = 1 + \left[3 \left(\frac{\sigma_s}{\sigma_f} - 1 \right) \phi / \left(\left(\frac{\sigma_s}{\sigma_f} + 2 \right) - \left(\frac{\sigma_s}{\sigma_f} - 1 \right) \phi \right) \right], \quad (3.7.4)$$

Where ρ_f density of base fluid, ρ_s is the density of the nanoparticles, ϕ is the volume fraction of the nanoparticles, μ_f is the density base fluid, σ_f is the electric conductivity of the base fluid, σ_s is the electric conductivity of the nanoparticles.

Magnetohydrodynamics Nanofluid Flow through Expanding or Contracting Channel with Permeable Walls

4.1 Introduction

Attained by dispersing and stably suspended nanoparticles into base water with typical dimensions of shape and size 1-100nm Choi(2007), Nanofluid is established as a new dynamic subclass of nanotechnology-based heat transfer fluids. Many researchers initiated their research on MHD Nanofluid flow through porous medium for its applications in technological and engineering sectors such as MHD generator; plasma studies, nuclear reactors, geothermal energy extraction. Akbar et al. (2016) studied heat and mass transfer analysis in a viscous unsteady MHD nanofluid flow through a channel with porous walls and medium in the presence of metallic nanoparticle. Elahi et al. (2014) researched theoretical study of blood flow of nanofluid through composite stenosed arteries with permeable walls. The problem of laminar nanofluid flow in a semi-porous channel in the presence of transverse magnetic field was investigated analytically by Sheikholeslami et al. (2013). Their results showed that velocity boundary layer thickness decreases with increases of Reynolds number and it increases as Hartmann number increases.

Majdalani et al. (2002) analyzed two dimensional viscous flows between slowly expanding, contracting walls with weak permeability. H.N. Chang et al (1989) studied velocity field of pulsatile flow in a porous tube. Their results found that Seepage across permeable walls is clearly important to the mass transfer between blood, air and tissue. Therefore, a substantial amount of research work has been invested in the study of the flow in rectangular domain bounded by two moving porous walls, which enable the fluid to enter or exit during successive expansions or contractions. Dauenhauer et al. (1999) studied the unsteady flow in semi-infinite expanding channels with wall injection. They characterized the two non-dimensional parameters, the expansion ratio of the wall and the cross-flow Reynolds number. Hatami et al. (2015) studied numerical analysis of nanofluid flow conveying nanoparticles through expanding and contracting gaps between permeable walls.

The present study of the research is to investigate the influence of magnetic field on nanofluid flow through expanding or contracting channel with permeable walls. The reduced

ordinary differential equations are solved using Hermite-Pade' approximation method. The bifurcation point of wall shear stress and velocity field are obtained due to wall dilation rate and the effects of physical governing parameters on velocity profile are also analyzed graphically.

4.2. Mathematical configuration

Considering the laminar unsteady and incompressible flow between two porous plates that enable the fluid to enter or exit during successive expansions or contractions shown in Figure 4.1. Water based different nanofluids are considered and assumed that the base fluid and the nanoparticles are in thermal equilibrium and no slip occurs between them. A uniform magnetic field B_0 is acting in direction normal to the right plate. The walls expand and contract uniformly at a time dependent rate $\bar{a} = \frac{da}{dt}$. The fluid inflow velocity is independent of position assumed to be V_w . A two-dimensional Cartesian coordinate system is considered and the flow is chosen along the x-axis.

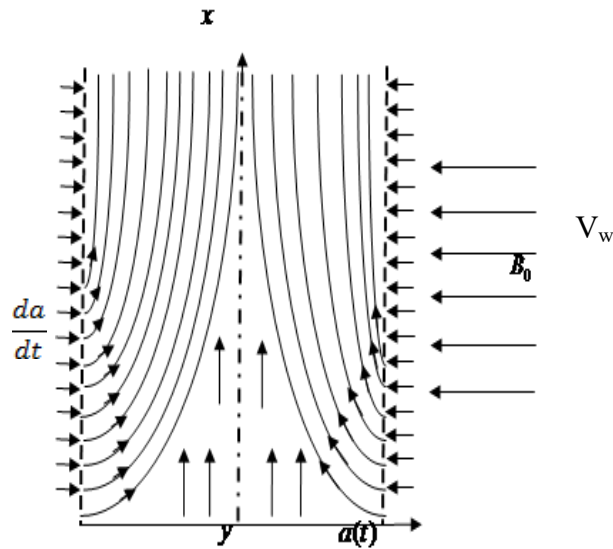


Fig: – 4.1 Physical configuration of the problem.

4.3 Physical properties

The thermo physical properties of different nanoparticles and base water are given:

Table 4.1: Thermo physical properties

Physical properties	Water	Al ₂ O ₃ (Alumina)	Ag (Silver)	Cu (Copper)
$\rho(kg/m^3)$	997.1	3970	10500	8933
$\mu(Pd/s)$	0.001	–	–	–
$\sigma(S/m)$	5.5×10^6	35×10^6	–	596×10^6

Here the symbol μ denotes dynamic viscosity, ρ denotes effective density and σ denotes effective electrical conductivity of the nanofluid.

4.4 Mathematical formulation

The continuity and momentum equations for the unsteady flow are as follows

$$\frac{\partial \bar{u}}{\partial x} + \frac{\partial \bar{v}}{\partial y} = 0 \quad (4.4.1)$$

$$\frac{\partial \bar{u}}{\partial t} + \bar{u} \frac{\partial \bar{u}}{\partial x} + \bar{v} \frac{\partial \bar{u}}{\partial y} = -\frac{1}{\rho_{nf}} \frac{\partial \bar{p}}{\partial x} + \frac{\mu_{nf}}{\rho_{nf}} \left[\frac{\partial^2 \bar{u}}{\partial x^2} + \frac{\partial^2 \bar{u}}{\partial y^2} \right] - \frac{\sigma_{nf} B_0^2 \bar{u}}{\rho_{nf}} \quad (4.4.2)$$

$$\frac{\partial \bar{v}}{\partial t} + \bar{u} \frac{\partial \bar{v}}{\partial x} + \bar{v} \frac{\partial \bar{v}}{\partial y} = -\frac{1}{\rho_{nf}} \frac{\partial \bar{p}}{\partial y} + \frac{\mu_{nf}}{\rho_{nf}} \left[\frac{\partial^2 \bar{v}}{\partial x^2} + \frac{\partial^2 \bar{v}}{\partial y^2} \right] \quad (4.4.3)$$

Where \bar{u} and \bar{v} are the velocity components in \bar{x} and \bar{y} directions, \bar{p} represents the dimensional pressure, t is the time, B_0 is the magnetic field intensity acting vertically downward on the right plate.

The boundary conditions are

$$\bar{u} = 0, \bar{v} = -V_w = -\frac{\bar{a}}{c} \quad \text{at} \quad \bar{y} = \bar{a}(t)$$

$$\begin{aligned}\frac{\partial \bar{u}}{\partial \bar{x}} = 0, \bar{v} = 0 & \quad \text{at } \bar{y} = 0 \\ \bar{v} = 0 & \quad \text{at } \bar{x} = 0\end{aligned}\tag{4.4.4}$$

and $c = \frac{V_w}{a}$ is the injection/ suction coefficient.

The stream functions and mean flow vorticity can be written as

$$\begin{aligned}\bar{u} = \frac{\partial \bar{\psi}}{\partial \bar{y}}, \bar{v} = -\frac{\partial \bar{\psi}}{\partial \bar{x}}, \bar{\xi} = \frac{\partial \bar{v}}{\partial \bar{x}} - \frac{\partial \bar{u}}{\partial \bar{y}} \\ \frac{\partial \bar{\xi}}{\partial \bar{t}} + \bar{u} \frac{\partial \bar{\xi}}{\partial \bar{x}} + \bar{v} \frac{\partial \bar{\xi}}{\partial \bar{y}} = \frac{\mu_{nf}}{\rho_{nf}} \left[\frac{\partial^2 \bar{\xi}}{\partial \bar{x}^2} + \frac{\partial^2 \bar{\xi}}{\partial \bar{y}^2} \right] - \frac{\sigma_{nf}}{\rho_{nf}} B_0^2 \frac{\partial \bar{u}}{\partial \bar{y}}\end{aligned}\tag{4.4.5}$$

Similarity variables are considered due to mass conservation as follows,

$$\bar{\psi} = \frac{v_{nf} \bar{x} \bar{f}(y, t)}{a}, \quad \bar{u} = \frac{v_{nf} \bar{x} \bar{f}_y}{a^2}, \quad \bar{v} = \frac{-v \bar{f}(y, t)}{a}, \quad y = \frac{\bar{y}}{a}, \quad \bar{f}_y = \frac{\partial \bar{f}}{\partial \bar{y}}\tag{4.4.6}$$

Substitution of Eq. (4.4.6) into Eq. (4.4.5) reduces to

$$u_{\bar{y}t} + \bar{u} \bar{u}_{\bar{y}\bar{x}} + \bar{v} \bar{u}_{\bar{y}\bar{y}} = v_{nf} \bar{u}_{\bar{y}\bar{y}\bar{y}} - \frac{\sigma_{nf}}{\rho_{nf}} B_0 \bar{u}_{\bar{y}}\tag{4.4.7}$$

The chain rule is used to solve Eqn. (4.4.7)

$$\bar{f}_{\bar{y}\bar{y}\bar{y}} + \alpha (\bar{y} \bar{f}_{\bar{y}\bar{y}} + 3 \bar{f}_{\bar{y}}) + \bar{f} \bar{f}_{\bar{y}\bar{y}} - \bar{f}_y \bar{f}_{\bar{y}} - \alpha^2 \left(\frac{\mu_{nf}}{\rho_{nf}} \right)^{-1} \bar{f}_{\bar{y}t} - \alpha^3 \left(\frac{\sigma_{nf}}{\mu_{nf}} \right) B_0 \bar{f}_{\bar{y}} = 0\tag{4.4.8}$$

With the following boundary conditions

$$\bar{f} = 0, \bar{f}_{\bar{y}} = 0 \quad \text{at } \bar{y} = 0$$

$$\text{and } \bar{f} = \text{Re}' A (1 - \phi)^{2.5}, \bar{f}_y = 0 \quad \text{at } \bar{y} = 1\tag{4.4.9}$$

Where $\alpha(t) \equiv \frac{\bar{a}\bar{a}'}{v_f}$ is the non-dimensional wall dilation rate, which is positive for expansion and

negative for contraction, $\text{Re}' = \frac{\rho_f \bar{a} V_w}{\mu_f}$ is the permeable Reynolds number and $Hd = B_0 \sqrt{\frac{\sigma_f}{\mu_f}}$ is

Hartmann number.

Equation (7), (9) and (10) can be normalized by taking

$$\psi = \frac{\bar{\psi}}{\alpha a}, u = \frac{\bar{u}}{a}, v = \frac{\bar{v}}{a}, f = \frac{\bar{f}}{\text{Re}AB} \quad (4.4.10)$$

and then $\psi = \frac{\mathcal{F}}{c}, u = \frac{x\mathcal{F}}{c}, v = \frac{-f}{c}, c = \frac{\alpha}{\text{Re}AB}$ (4.4.11)

$$f^{iv} + \alpha(\mathcal{F}^{iii} + 3f^{ii}) + \text{Re}' AB(f^{iii} - f^i f^{ii}) - Ha^2 C f^{ii} = 0 \quad (4.4.12)$$

Boundary conditions (10) is reduced to

$$y=0: f=0, f^{ii}=0 \quad \text{and} \quad y=1: f=1, f^i=0 \quad (4.4.13)$$

$$A = (1-\phi) + \frac{\rho_s}{\rho_f} \phi, \quad B = (1-\phi)^{2.5}, \quad C = 1 + \left[3 \left(\frac{\sigma_s}{\sigma_f} - 1 \right) \phi / \left(\left(\frac{\sigma_s}{\sigma_f} + 2 \right) - \left(\frac{\sigma_s}{\sigma_f} - 1 \right) \phi \right) \right]$$
 are the constants.

For normalization, substituting $\text{Re} = \frac{\text{Re}'}{\alpha}$ and $Ha = \frac{Ha'}{\alpha}$ into equation (13) becomes

$$f^{iv} + \alpha(\mathcal{F}^{iii} + 3f^{ii}) + \alpha \text{Re} AB(f^{iii} - f^i f^{ii}) - \alpha Ha^2 C f^{ii} = 0 \quad (4.4.14)$$

Another important quantity is the shear stress. Shear stress can be determined from Newton's law for viscosity:

$$\tau = \mu_f (v_x + u_y) = \frac{\rho_f \nu^2 \mathcal{F}^{ii}}{\alpha^3} \quad (4.4.15)$$

Introducing non-dimensional shear stress $\tau = \frac{\tau}{\rho_f V_w^2} W$, we have

$$\tau = \frac{\mathcal{F}^{ii}}{\text{Re}AB} \quad (4.4.16)$$

4.5 Series analysis

A power series considered in terms of α in the following form as equation (15) is non-linear

$$f(y) = \sum_{k=0}^{\infty} f_k \alpha^k \quad (4.5.1)$$

Substituting the equation (4.5.1) into equation (4.4.14) and equating the coefficient of power series α , with the help of MAPLE, we have computed the first 13 coefficients for the series of the stream function $f(y)$. The first few coefficients of the series of $f(y)$ are as follows:

$$\begin{aligned}
 f(y, Re, Ha, A, B, C, \alpha) = & \frac{3}{2}y - \frac{1}{2}y^3 + \left(\left(\frac{1}{140} ReAB + \frac{1}{10} - \frac{1}{40} Ha^2 C \right) y + \left(-\frac{1}{5} + \frac{1}{20} Ha^2 C - \frac{3}{280} ReAB \right) y^3 + \right. \\
 & \left. \left(\frac{1}{10} - \frac{1}{40} Ha^2 C \right) y^5 + \frac{1}{280} ReAB y^7 \right) \alpha + \left(\left(\frac{2}{175} - \frac{17}{2100} Ha^2 C - \frac{703}{1293600} Re^2 A^2 B^2 - \frac{37}{4200} ReAB + \frac{23}{11200} ReAB Ha^2 C + \right. \right. \\
 & \left. \left. \frac{11}{8400} Ha^4 C \right) y + \left(-\frac{13}{350} + \frac{31}{350} Ha^2 C + \frac{73}{107800} Re^2 A^2 B^2 + \frac{37}{3150} ReAB - \frac{23}{8400} ReABCHa - \frac{9}{2800} Ha^4 C \right) y^3 + \right. \\
 & \left. \left(-\frac{3}{5600} ReABCHa - \frac{1}{50} Ha^2 + \frac{3}{1400} ReAB + \frac{1}{100} Ha^4 C + \frac{1}{25} \right) y^5 + \left(-\frac{3}{700} ReAB + \frac{3}{19600} Re^2 A^2 B^2 - \frac{1}{70} + \right. \right. \\
 & \left. \left. \frac{1}{1680} Ha^4 C + \frac{3}{2800} ReABCHa \right) y^7 + \left(\frac{-1}{1260} ReAB - \frac{1}{3360} Re^2 A^2 B^2 + \frac{1}{6720} ReABCHa \right) y^9 + \frac{1}{92400} Re^2 A^2 B^2 y^{11} \right) \alpha^2 \\
 & + O(\alpha^3)
 \end{aligned}
 \tag{4.5.2}$$

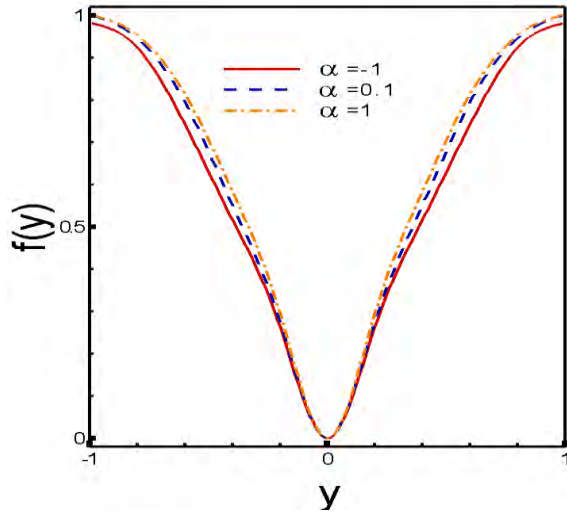
The series is then analyzed by using various form of Approximation method.

4.6. Results and discussion

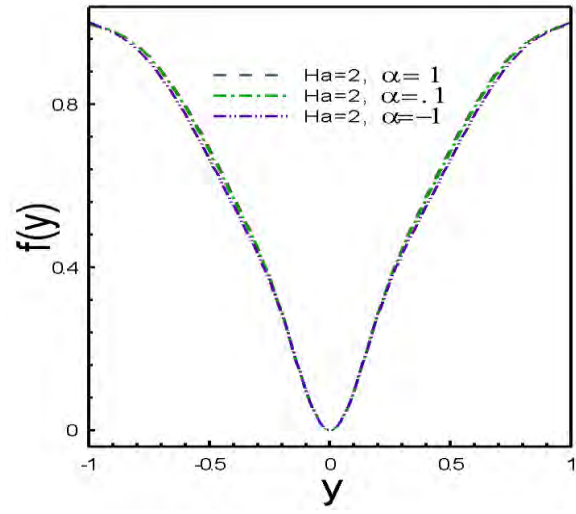
By differentiating the series (4.5.2), we have computed the velocity function f' as a series in power α , Re and Ha respectively. To apply Hermite-Pade` approximation method to obtain an explicit solution of laminar unsteady incompressible different nanofluid in a parallel channel bounded by two moving porous walls, which enable the nanofluid to enter or exit due to successive expansion or contractions.

Fig: 4.2(a) and Fig: 4.2(b) is showing the effect of non dimensional wall dilation rate α on stream function and fluid velocity respectively. The fluid velocity increases along the centerline with the positively increasing values of dimensionless wall dilation rate due to successive expansion of channel width. On the other hand, velocity decreases at the centre of the channel whereas increases near the two plates when α decreases negatively. The magnetic field has a significant effect on the velocity profile with the variation of α . Fig: 4.3(a) and Fig: 4.3(b) have shown the effect of nanoparticles volume fraction on stream function and velocity profiles respectively. As nanoparticles volume fraction increases, fluid velocity $f'(y)$ also increases while the stream function $f(y)$ decreases. It can be seen from Fig: 4.4(a) and fig: 4.4(b) that fluid centerline velocity reduces while increases near the two walls by the decreasing values of

permeation Reynolds number Re . It is also shown that in absence of Hartmann number stream function $f(y)$ increases slightly while velocity $f'(y)$ increases sharply.



Reproduced Hatami et al.(2015) Results



Present Results

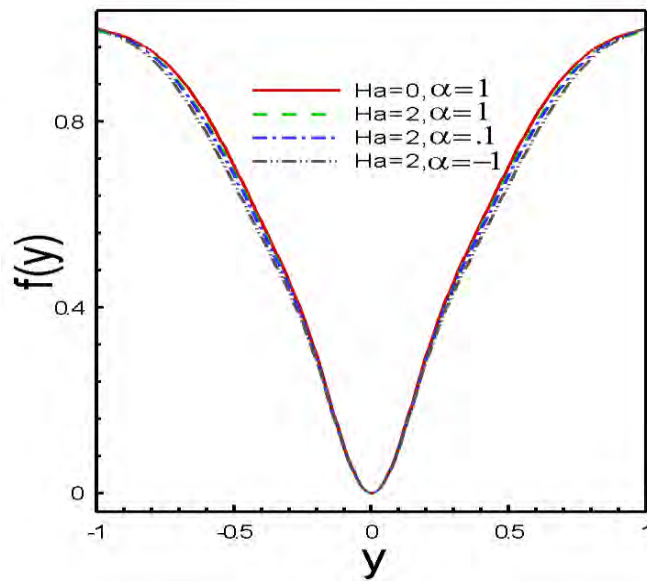
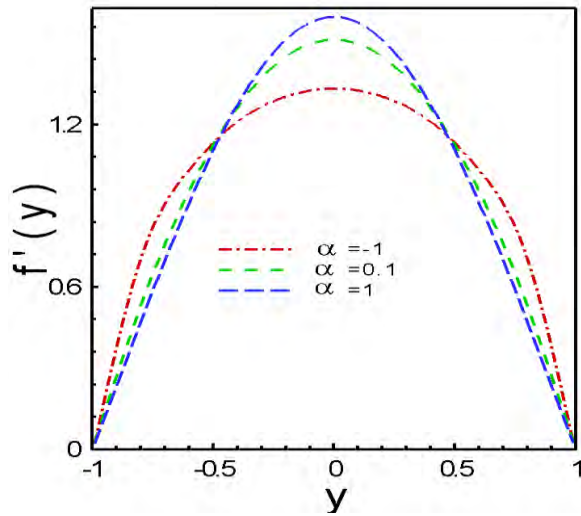
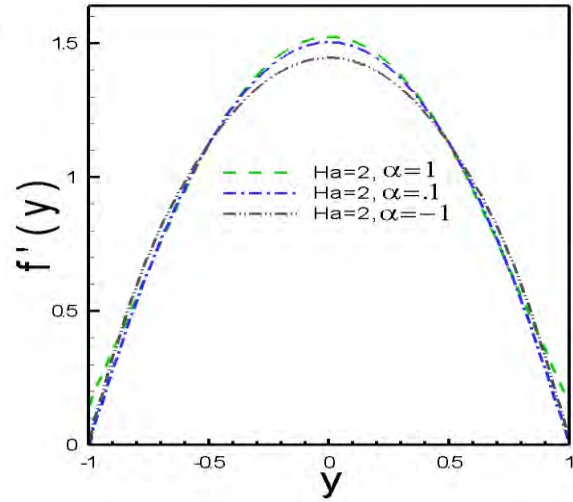


Fig:- 4.2(a) Non-dimensional wall dilation rate effect on stream function and comparison.



Reproduced Hatami et al. (2015) Results



Present Results

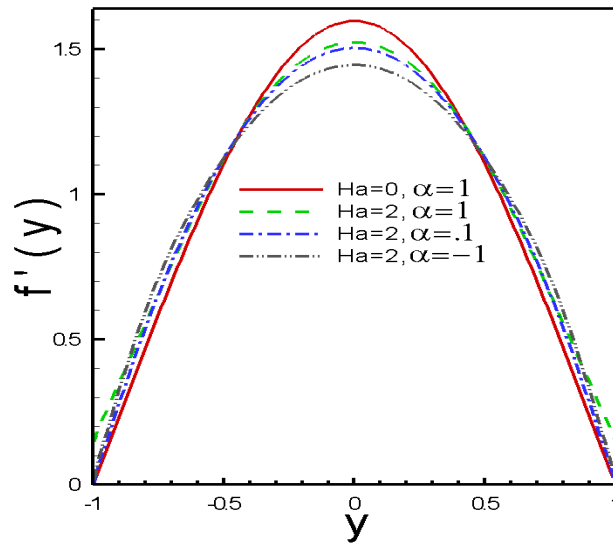
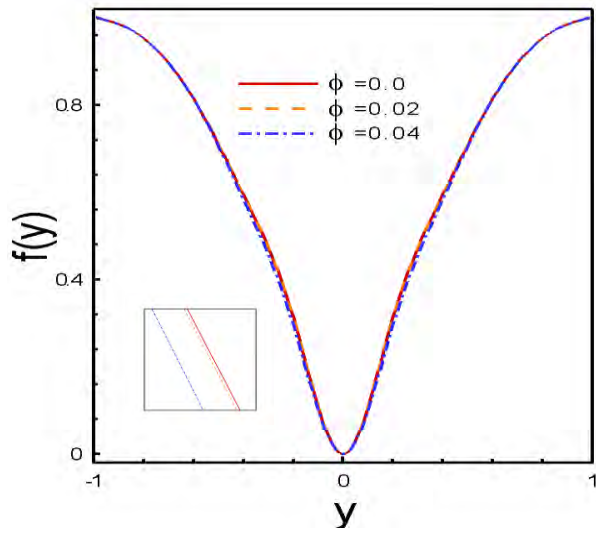
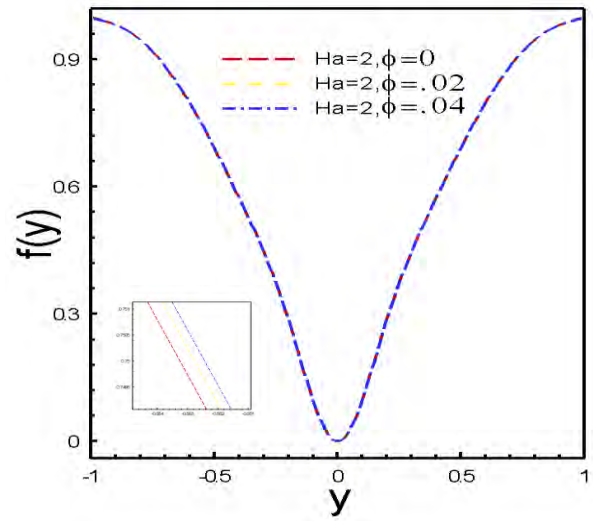


Fig:- 4.2(b) Non-dimensional wall dilation rate effect on velocity profile and comparison.



Reproduced Hatami et al. (2015) Results



Present Results

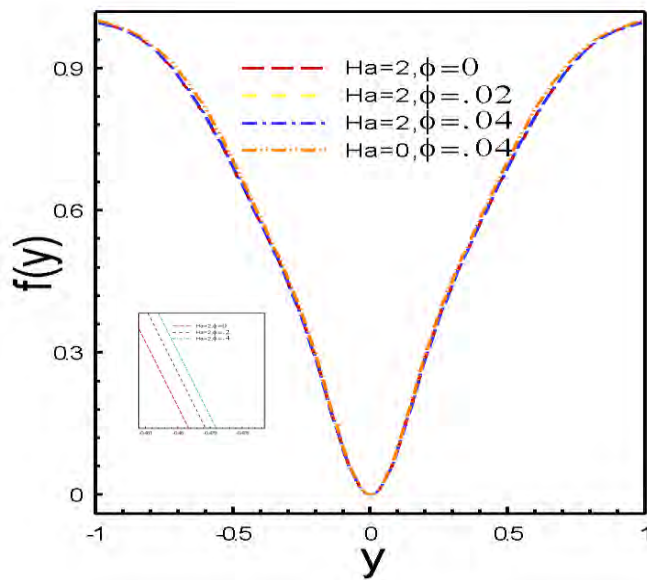
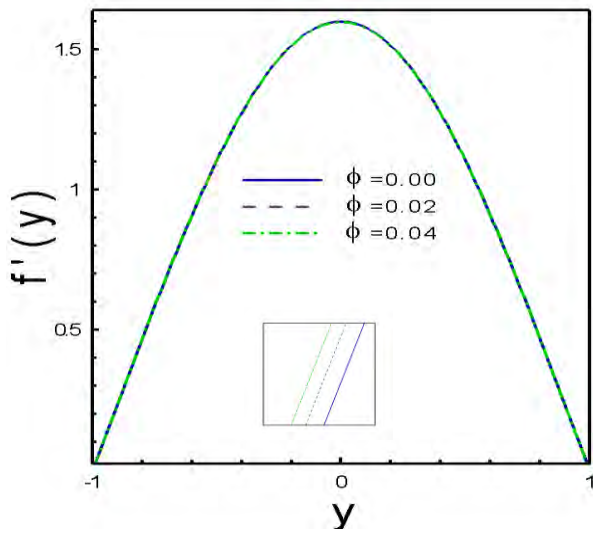
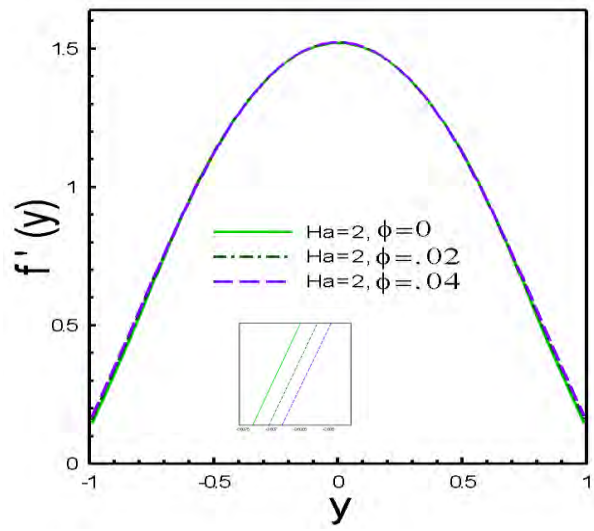


Fig:- 4.3(a) Nanoparticles volume fraction effect on stream function and comparison.



Reproduced Hatami et al. (2015) Results



Present Results

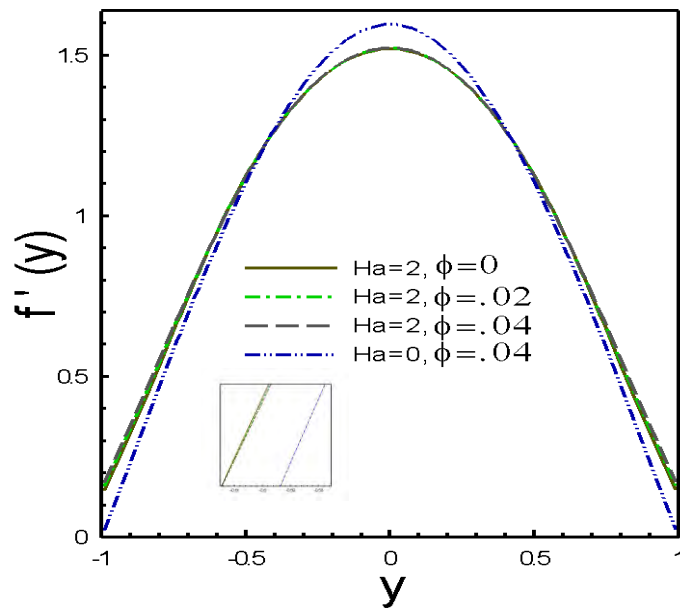
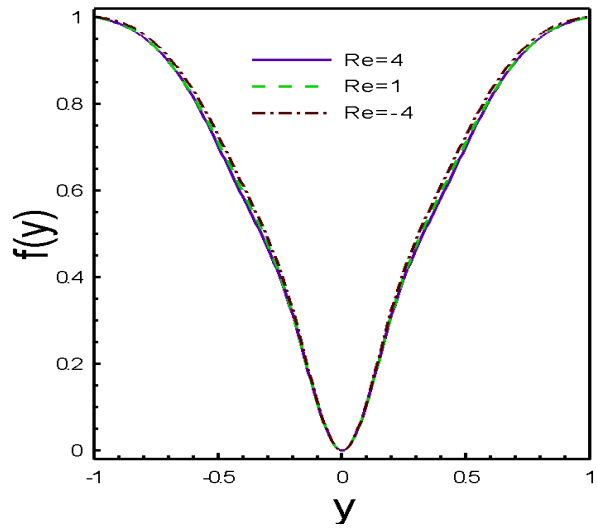
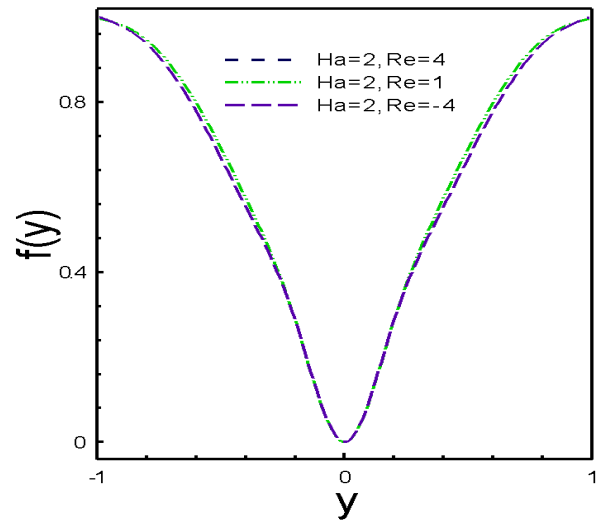


Fig:- 4.3(b) Nanoparticles volume fraction effect on velocity profile and comparison.



Reproduced Hatami et al. (2015) Results



Present Results

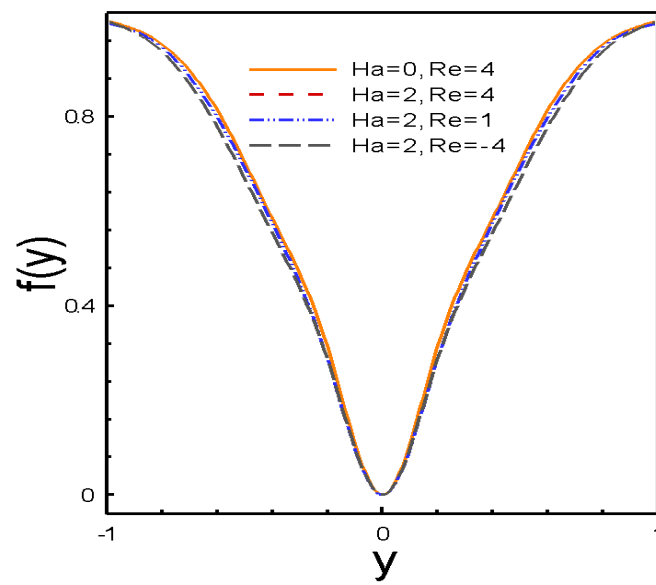
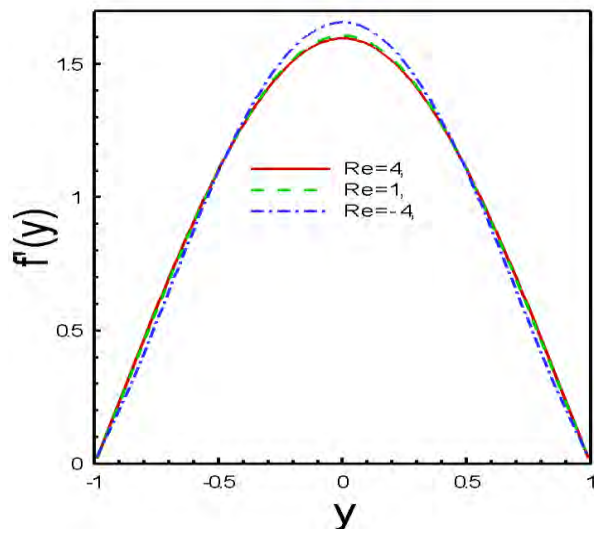
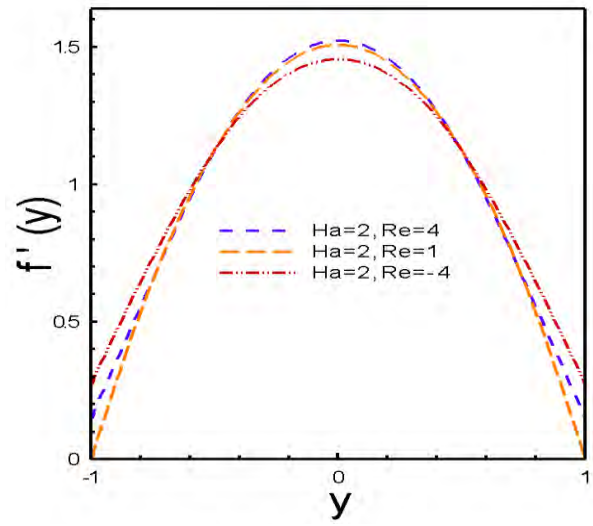


Fig:- 4.4(a) Reynolds number effect on stream function and comparison.



Reproduced Hatami et al. (2015) Results



Present Results

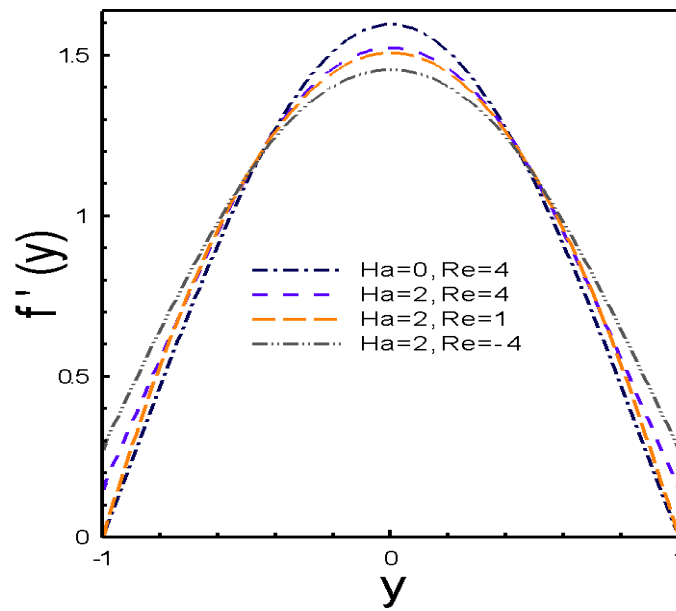
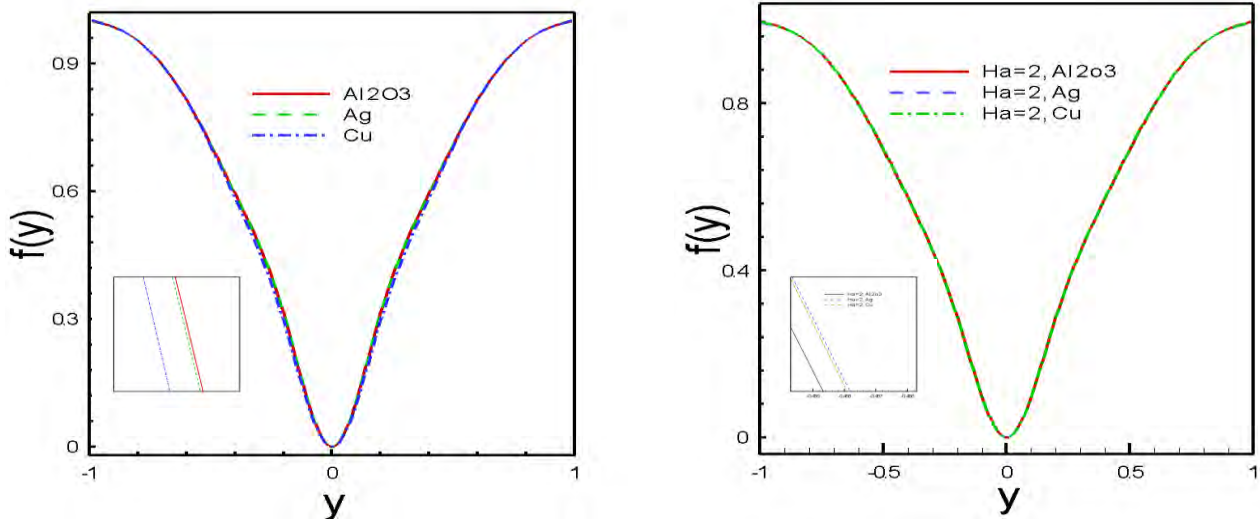


Fig:- 4.4(b) Reynolds number effect on velocity profile and comparison.

The effects of different nanoparticles volume fraction on $f(y)$ and $f'(y)$ are noticed in Fig 4.5(a) and 4.5(b). It shows that the Ag-nanoparticles produce larger horizontal velocity near the walls. Moreover, Cu-nanoparticles enhance centerline velocity in absence of magnetic field.



Reproduced Hatami et al. (2015) Results

Present Results

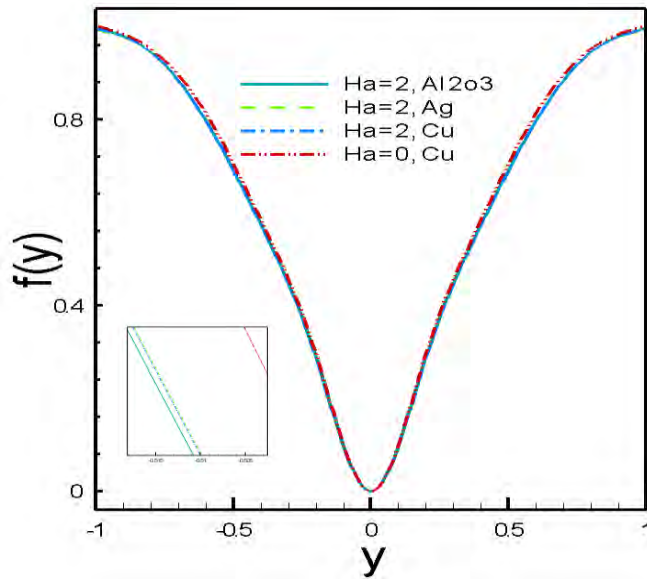
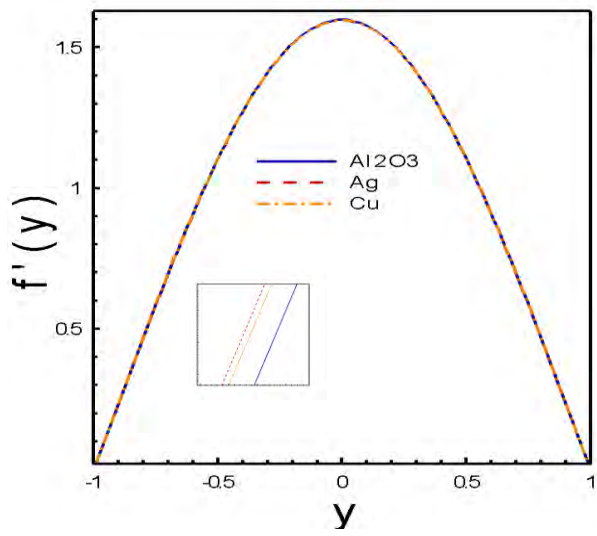
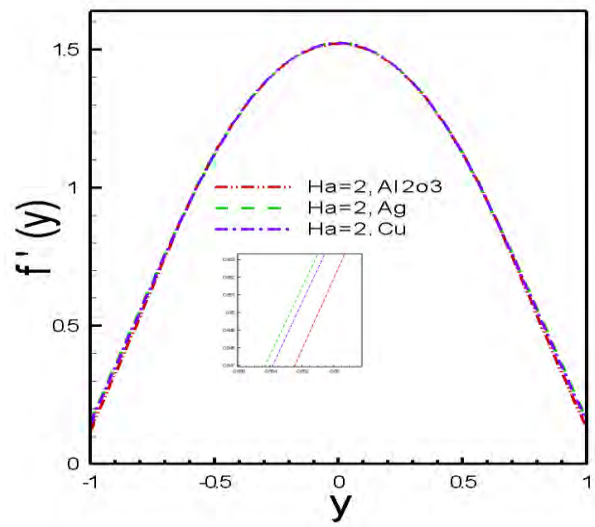


Fig:- 4.5(a) Nanoparticles volume fraction effect on stream function and comparison.



Reproduced Hatami et al. (2015) Results



Present Results

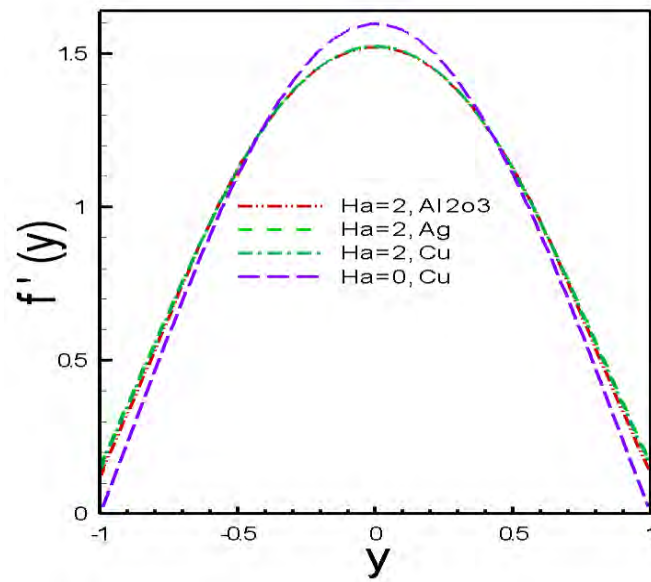
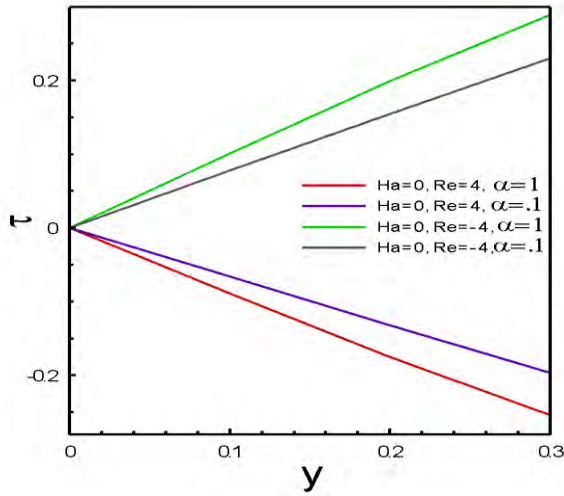
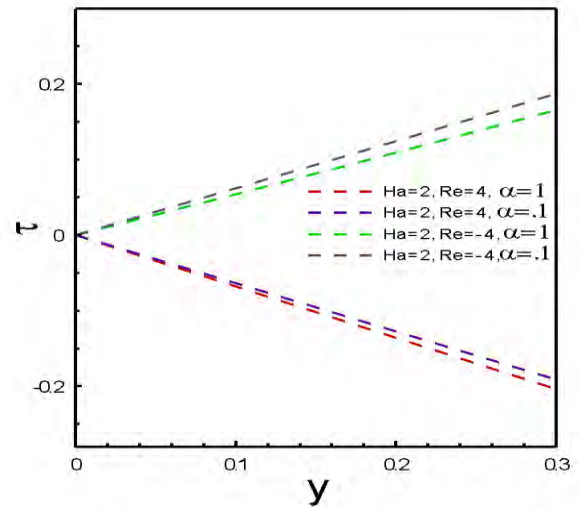


Fig:- 4.5(b) Nanoparticles volume fraction effect on velocity profile and comparison.

The wall shear stress for different values of permeable Reynolds number over a range of non-dimensional wall dilation rate and Hartmann number are represented in Fig 4.6. The absolute value of shear stress decreases when the non-dimensional wall dilation rate increases. Moreover, it is also noticed that the wall shear stress decreases rapidly by the positive variation of Ha .



Reproduced Hatami et al. (2015) Results



Present Results

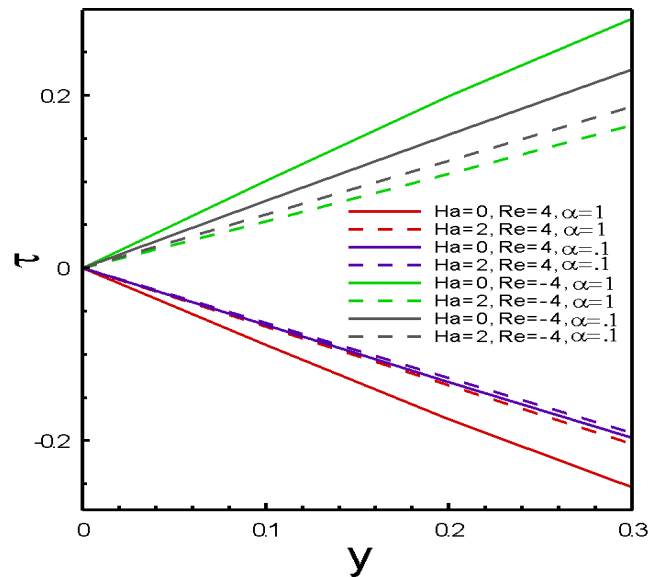
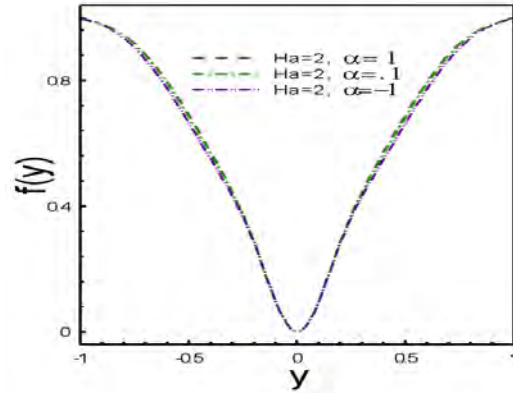


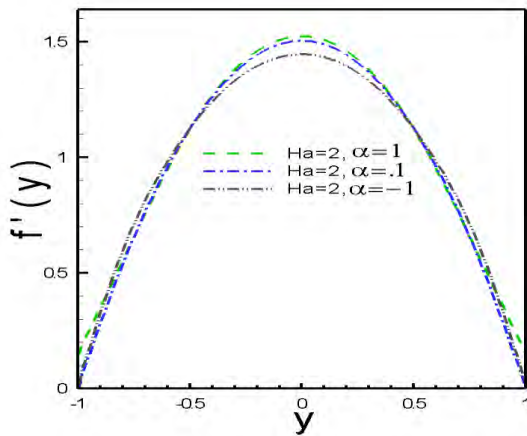
Fig:- 4.6 Shear stress for different parameters

4.7 Special case study:

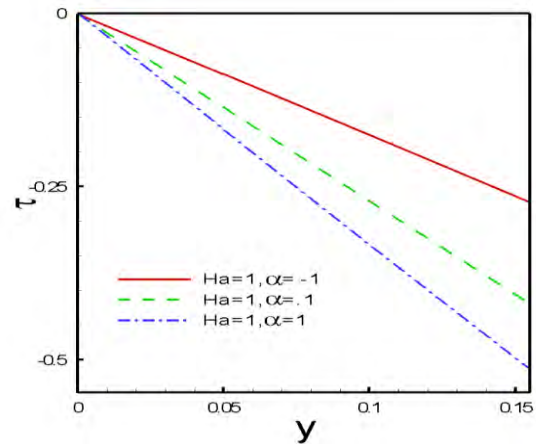
Section (A): Stability of MHD Cu- water based nanofluid flow through expanding and contracting channel with permeable wall.



(a)



(b)



(c)

Fig:- 4.7(A)-1 (a) Stream function (b) Velocity profile (c) Shear stress for cu- water based nanofluid flow for different value of α , where $Re = 1$; $Ha= 1, 2$; $\Phi = 0.04$.

Fig: (a), Fig: (b) and Fig: (c) show the effects of non-dimensional wall dilation rate α on stream function, fluid velocity and shear stress respectively. The fluid velocity increases along the centerline with the positively increasing values of dimensionless wall dilation rate due to successive expansion of channel width. On the other hand, velocity decreases at the centre of the channel whereas increases near the two plates when α decreases negatively. The absolute value

of shear stress decreases when the non-dimensional wall dilation rate increases. The magnetic field has a significant effect on the velocity profile with the variation of α .

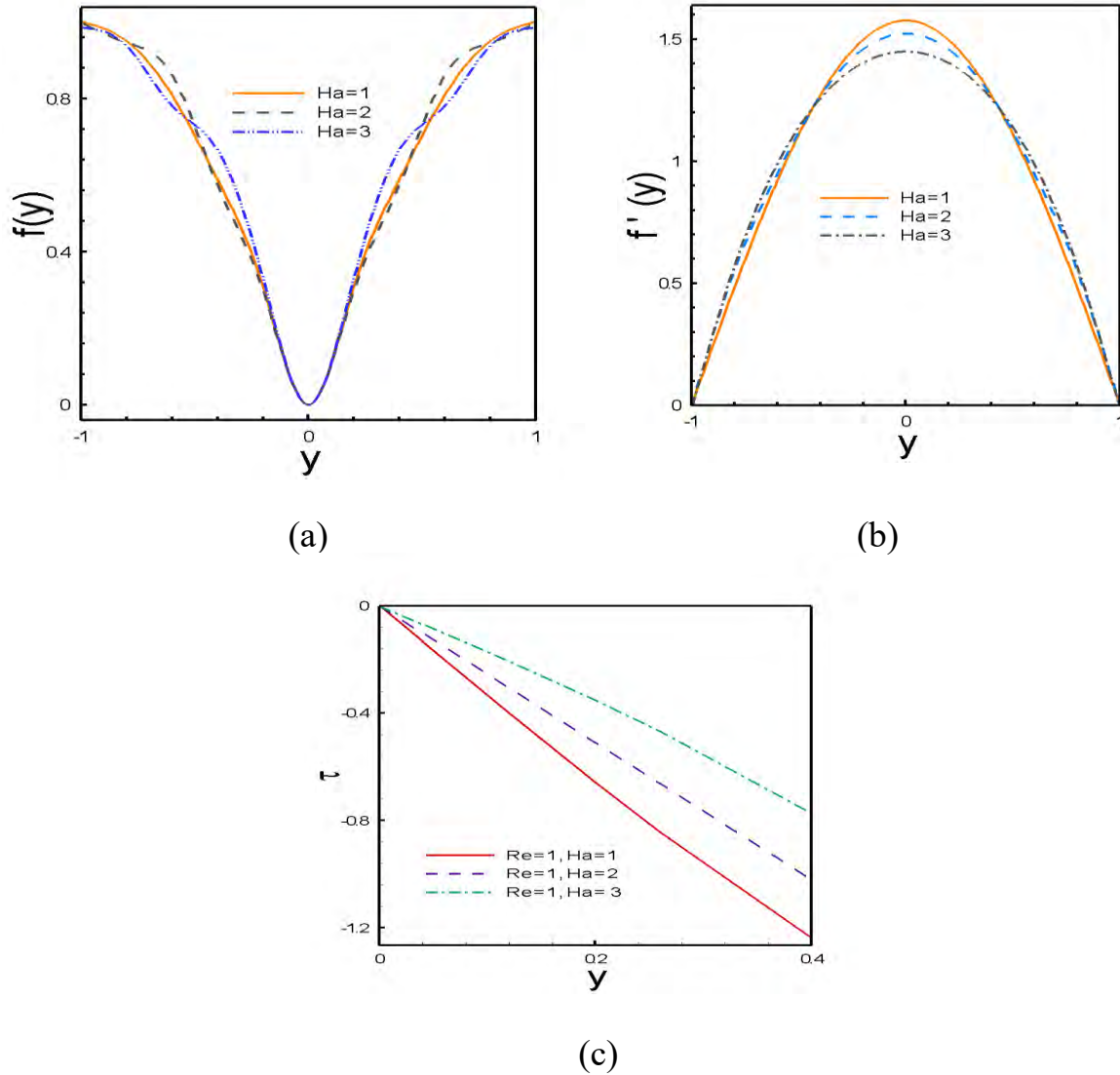


Fig:- 4.7(A)-2 (a) Stream function (b) Velocity profile (c) Shear stress for cu- water based nanofluid flow for different value of Ha , where $Re = 1$; $\alpha = 1$; $\Phi = 0.04$.

Fig: (a), Fig: (b) and Fig: (c) show the effects of Hartmann number on stream function, fluid velocity and shear stress respectively. It is seen that velocity at the centre of the channel reduces while enhances around the two plates when Ha increases. The transverse magnetic field opposes the alteration phenomena clearly. Because the variation of Ha leads to the variation of the

Lorentz force due to magnetic field and the Lorentz force produces more resistance to the alternation phenomena. The stream function is fluctuated while Hartmann number Ha increases. The absolute value of shear stress increases when Hartmann number increases.

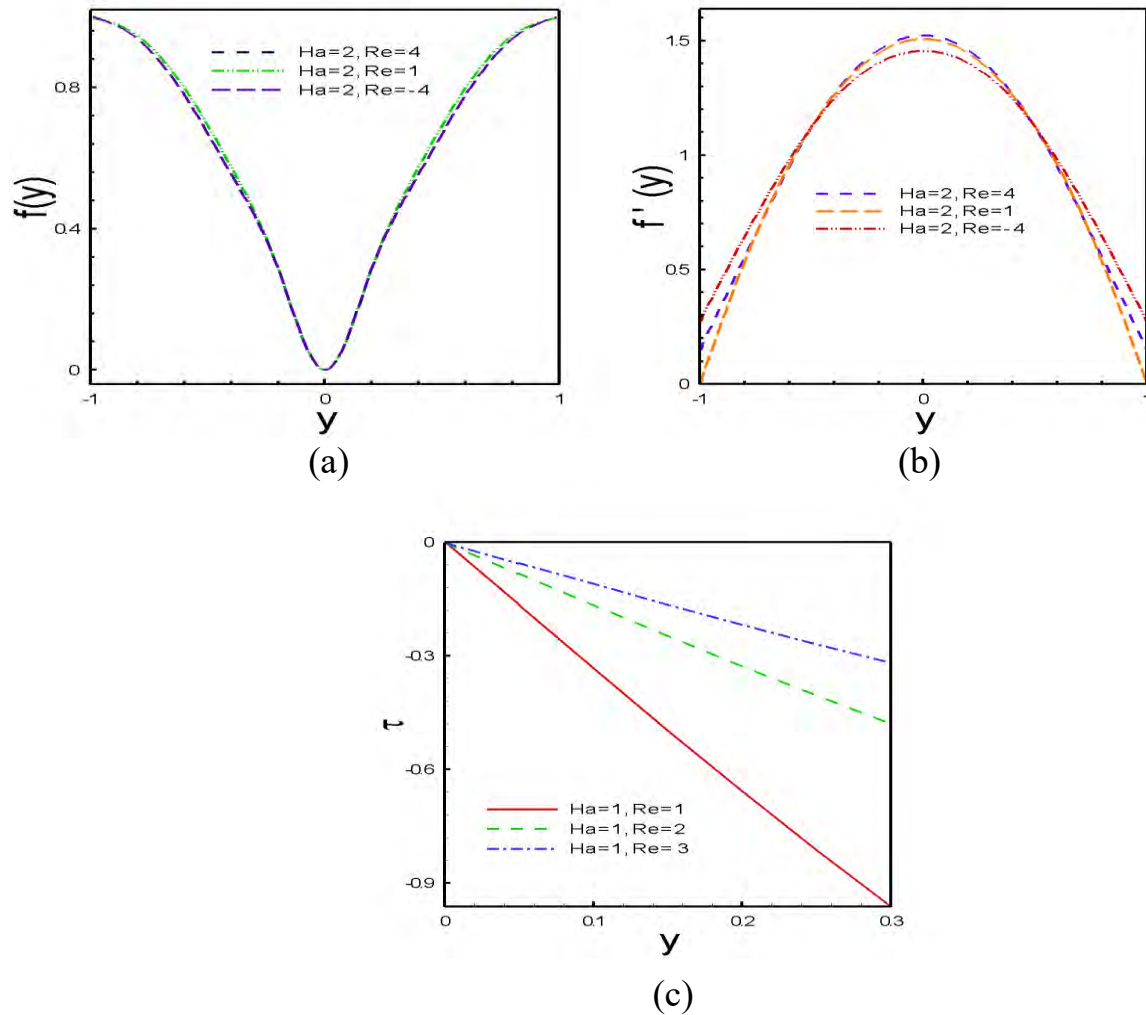
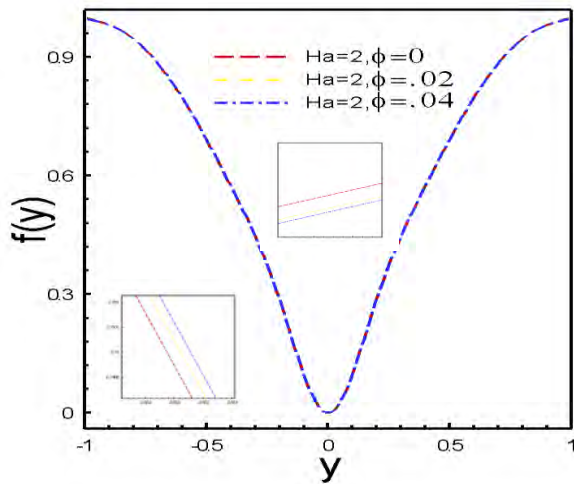
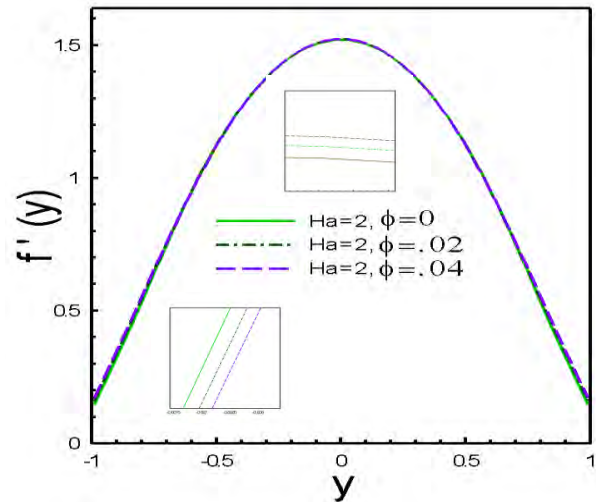


Fig:- 4.7(A)-3 (a) Stream function (b) Velocity profile (c) Shear stress for cu- water based nanofluid flow for different value of Re , where $\alpha = 1$; $Ha= 1, 2$; $\Phi = 0.04$.

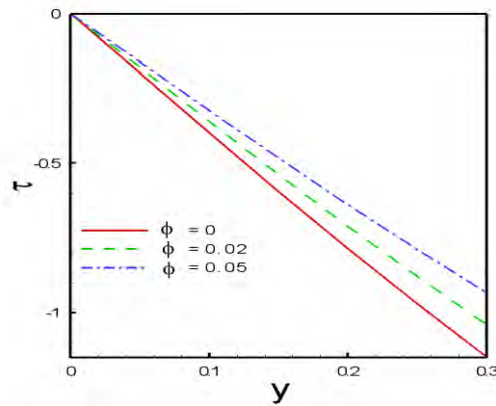
Fig: (a), Fig: (b) and Fig : (c) show the effects Reynolds number on stream function, fluid velocity and shear stress respectively. It can be seen from Fig: (a) and Fig: (b) that fluid centerline velocity reduces while increases near the two walls by the decreasing values of permeation Reynolds number Re . Fig: (c) shows that the absolute value of shear stress increases when Reynolds number increases.



(a)



(b)



(c)

Fig:- 4.7(A)-4 (a) Stream function (b) Velocity profile (c) Shear stress for cu- water based nanofluid flow for different value of Φ , where $\alpha = 1$; $Ha = 1, 2$; $Re = 1$.

Fig: (a), Fig: (b) and Fig: (c) show the effects of Nanoparticle on stream function, fluid velocity and shear stress respectively. As nanoparticles volume fraction increases, the value of fluid velocity $f'(y)$ at the centre of the channel increases also around the two plates while the value of stream function $f(y)$ increases at the centre of the channel while decreases around the two plates. The absolute value of shear stress increases when nanoparticles volume fraction increases.

Table 4.2: Significant differences among different value of Φ for cu- water based nanofluid:

Value of y	Value of $f(y)$			Value of $f'(y)$		
	$\Phi=0.0$	$\Phi=0.02$	$\Phi=0.04$	$\Phi=0.0$	$\Phi=0.02$	$\Phi=0.04$
y = 0	0.000000e-01	0.000000e-01	0.000000e-01	1.520104e+00	1.521615e+00	1.522859e+00
y = ± 0.2	2.887321e-01	2.878144e-01	2.875581e-01	1.456301e+00	1.457512e+00	1.458506e+00
y = ± 0.4	5.740328e-01	5.744740e-01	5.747508e-01	1.265290e+00	1.265640e+00	1.265922e+00
y = ± 0.6	7.975802e-01	7.979769e-01	7.983003e-01	9.502829e-01	9.495213e-01	9.488938e-01
y = ± 0.8	9.462312e-01	9.463118e-01	9.463629e-01	5.343879e-01	5.444338e-01	5.534769e-01
y = ± 0.99	9.974374e-01	9.967364e-01	9.960567e-01	1.471616e-01	1.601279e-01	1.712881e-01

From table, it is shown that as nanoparticles volume fraction increases, the value of fluid velocity $f'(y)$ at the centre of the channel increases also around the two plates while the value of stream function $f(y)$ increases at the centre of the channel while decreases around the two plates.

Section (B): Stability of MHD Ag- water based nanofuid flow through expanding and contracting channel with permeable wall.

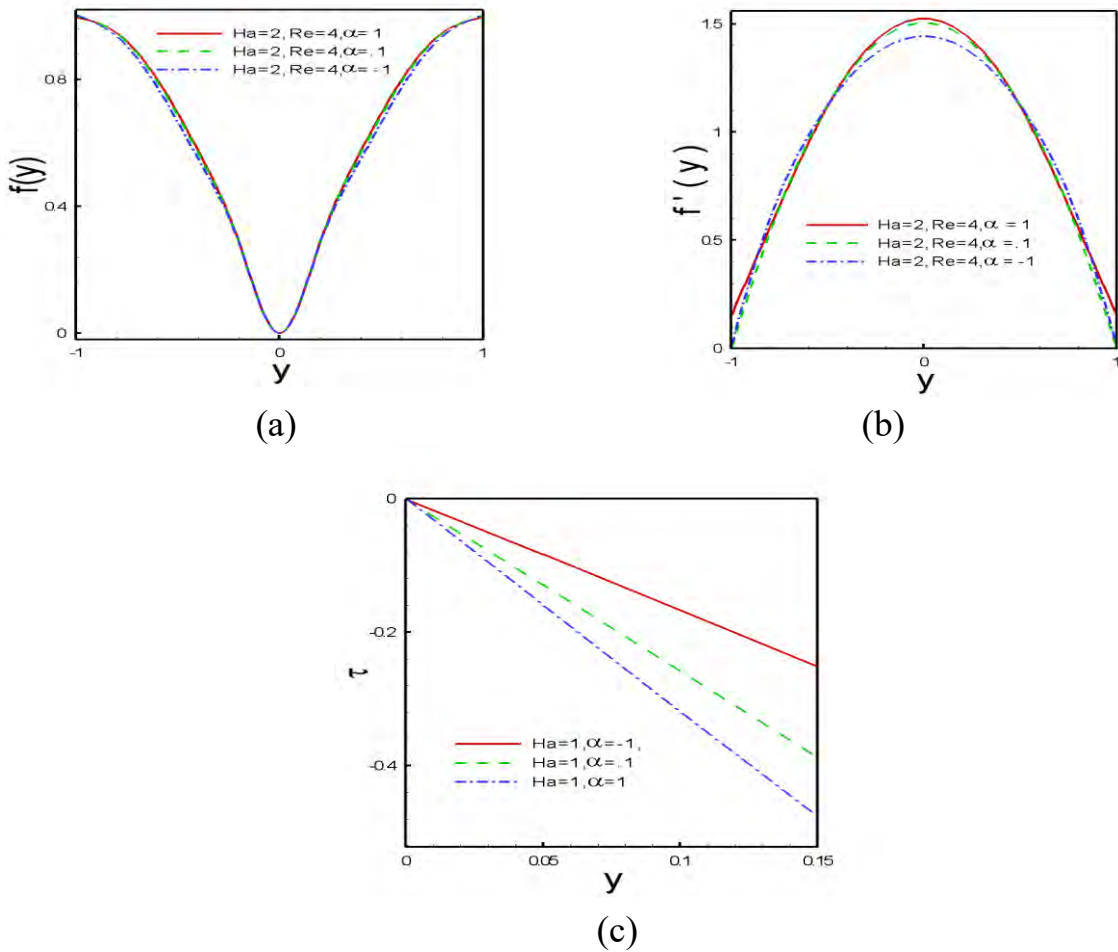
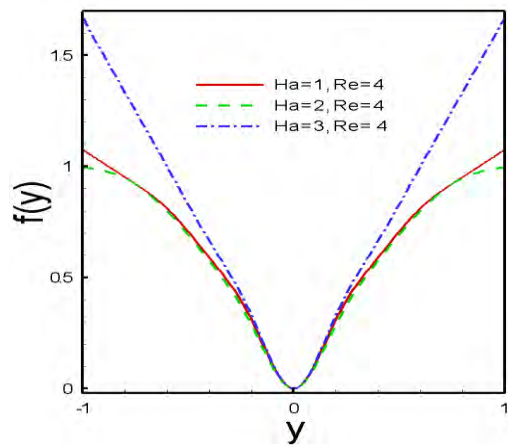
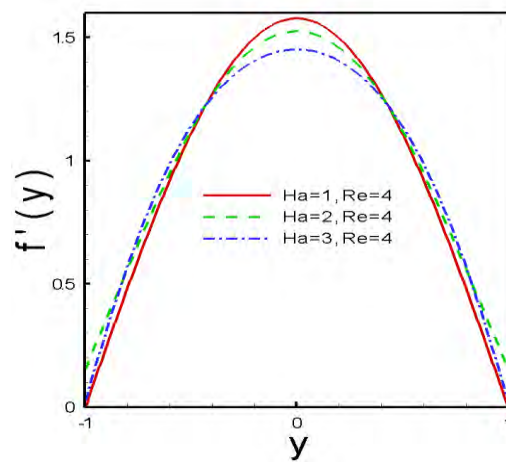


Fig:- 4.7(B)-1 (a) Stream function (b) Velocity profile (c) Shear stress for Ag - water based nanofuid flow for different value of α , where $\Phi = 0.04$; $Ha= 1, 2$; $Re = 1, 4$.

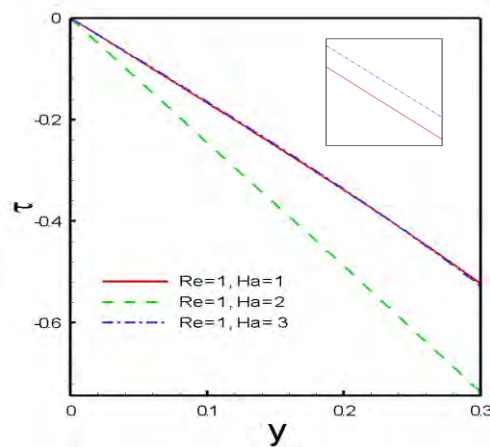
Fig: (a), Fig: (b) and Fig: (c) show the effects of non-dimensional wall dilation rate α on stream function, fluid velocity and shear stress respectively. The fluid velocity increases along the centerline with the positively increasing values of dimensionless wall dilation rate due to successive expansion of channel width. On the other hand, velocity decreases at the centre of the channel whereas increases near the two plates when α decreases negatively. The absolute value of shear stress decreases when the non-dimensional wall dilation rate increases. The magnetic field has a significant effect on the velocity profile with the variation of α .



(a)



(b)



(c)

Fig:- 4.7(B)-2 (a) Stream function (b) Velocity profile (c) Shear stress for Ag - water based nanofluid flow for different value of Ha , where $\alpha = 1$; $Re = 1, 4$; $\Phi = 0.04$.

Fig: (a), Fig: (b) and Fig: (c) show the effects of Hartmann number on stream function, fluid velocity and shear stress respectively. It is seen that velocity at the centre of the channel reduces while enhances around the two plates when Ha increases. The transverse magnetic field opposes the alteration phenomena clearly. Because the variation of Ha leads to the variation of the Lorentz force due to magnetic field and the Lorentz force produces more resistance to the alternation phenomena. The stream function is increases while Hartmann number Ha increases.

The absolute value of shear stress decreases primarily then increases when Reynolds number is positive as well as Hartmann number increases.

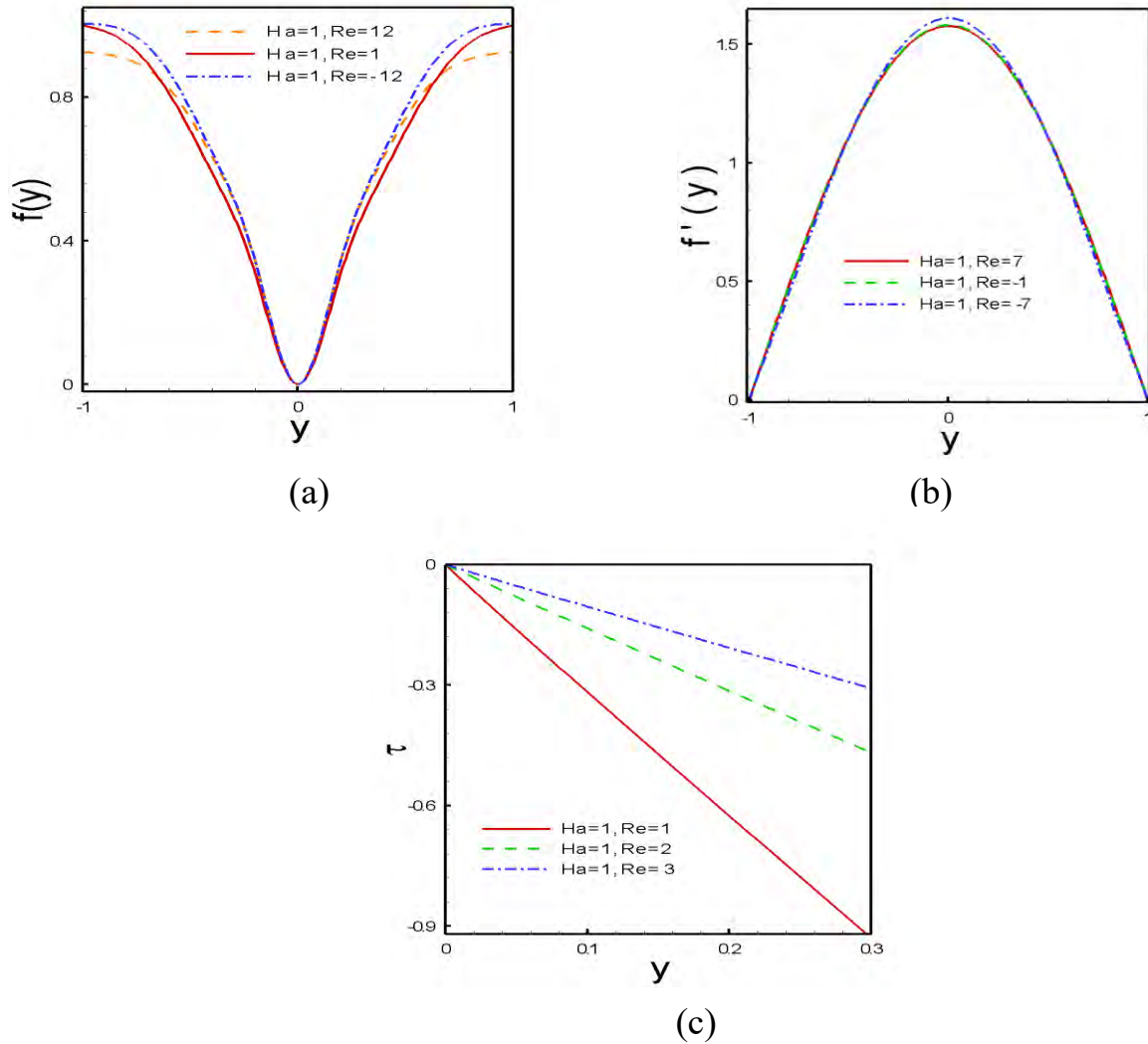
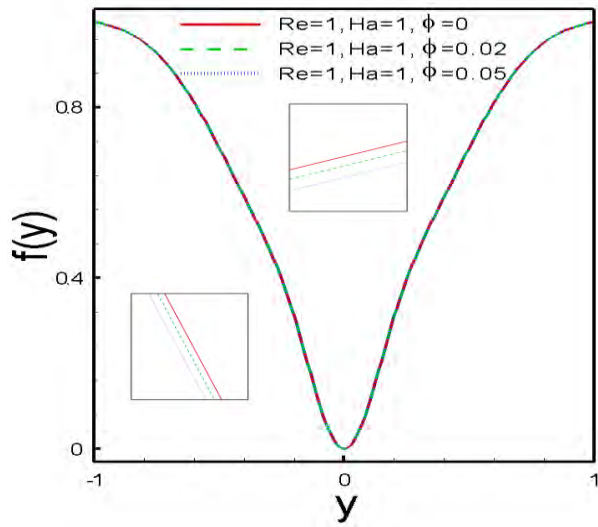
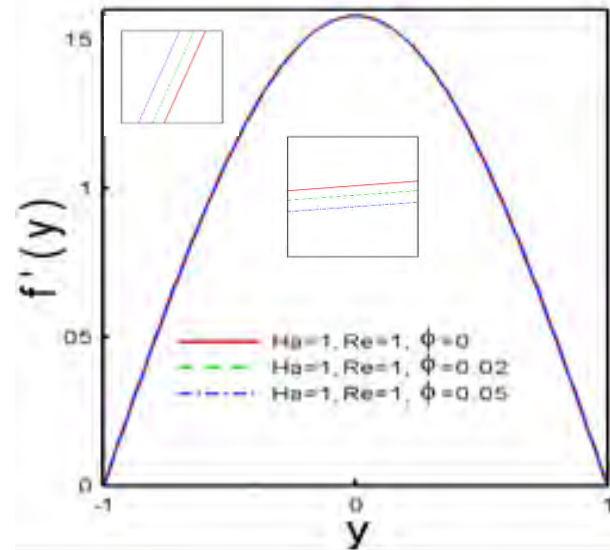


Fig:- 4.7(B)-3 (a) Stream function (b) Velocity profile (c) Shear stress for Ag – water based nanofluid flow for different value of Re , where $\alpha = 1$; $Ha = 1$; $\Phi = 0.04$.

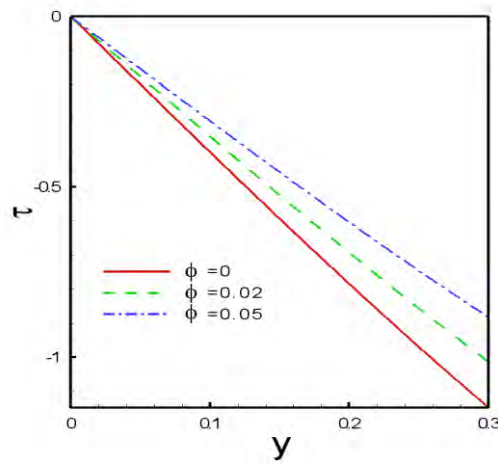
Fig: (a), Fig: (b) and Fig: (c) show the effects of Reynolds number on stream function, fluid velocity and shear stress respectively. It can be seen from Fig: (a) and Fig: (b) that fluid centerline velocity reduces while increases near the two walls by the decreasing values of permeable Reynolds number Re . Fig: (c) shows that the absolute value of shear stress increases when Reynolds number increases.



(a)



(b)



(c)

Fig:- 4.7(B)-4 (a) Stream function (b) Velocity profile (c) Shear stress for Ag – water based nanofluid flow for different value of Φ , where $\alpha = 1$; $Re = 1$; $Ha = 1$.

Fig: (a), Fig: (b) and Fig: (c) show the effect of nanoparticle on stream function, fluid velocity and shear stress respectively. As nanoparticles volume fraction increases, fluid velocity $f'(y)$ at the centre of the channel reduces while enhances around the two plates while the value of stream function $f(y)$ decreases. The absolute value of shear stress increases when nanoparticles volume fraction increases.

Table 4.3: Significant differences among different values of Φ for Ag- water based nanofluid:

Value of y	Value of $f(y)$			Value of $f'(y)$		
	$\Phi=0.0$	$\Phi=0.02$	$\Phi=0.05$	$\Phi=0.0$	$\Phi=0.02$	$\Phi=0.05$
y = 0	0.000000e-01	0.000000e-01	0.000000e-01	1.578552e+00	1.578429e+00	1.578280e+00
y = ± 0.2	3.104048e-01	3.103822e-01	3.103544e-01	1.499286e+00	1.499191e+00	1.499074e+00
y = ± 0.4	5.897256e-01	5.896906e-01	5.896479e-01	1.270756e+00	1.270734e+00	1.270709e+00
y = ± 0.6	8.104559e-01	8.104257e-01	8.103889e-01	9.188524e-01	9.189192e-01	9.190011e-01
y = ± 0.8	9.515264e-01	9.515139e-01	9.514985e-01	4.810668e-01	4.811639e-01	4.812819e-01
y = ± 1.0	9.999651e-01	9.999613e-01	9.999568e-01	8.482054e-06	6.225556e-06	1.998789e-06

From the table it is seen that, as nanoparticles volume fraction increases, the value of fluid velocity $f'(y)$ at the centre of the channel reduces while increases around the two plates while the value of stream function $f(y)$ decreases.

Section(C): Stability of MHD Al_2O_3 - water based nanofluid flow through expanding and contracting channel with permeable wall.

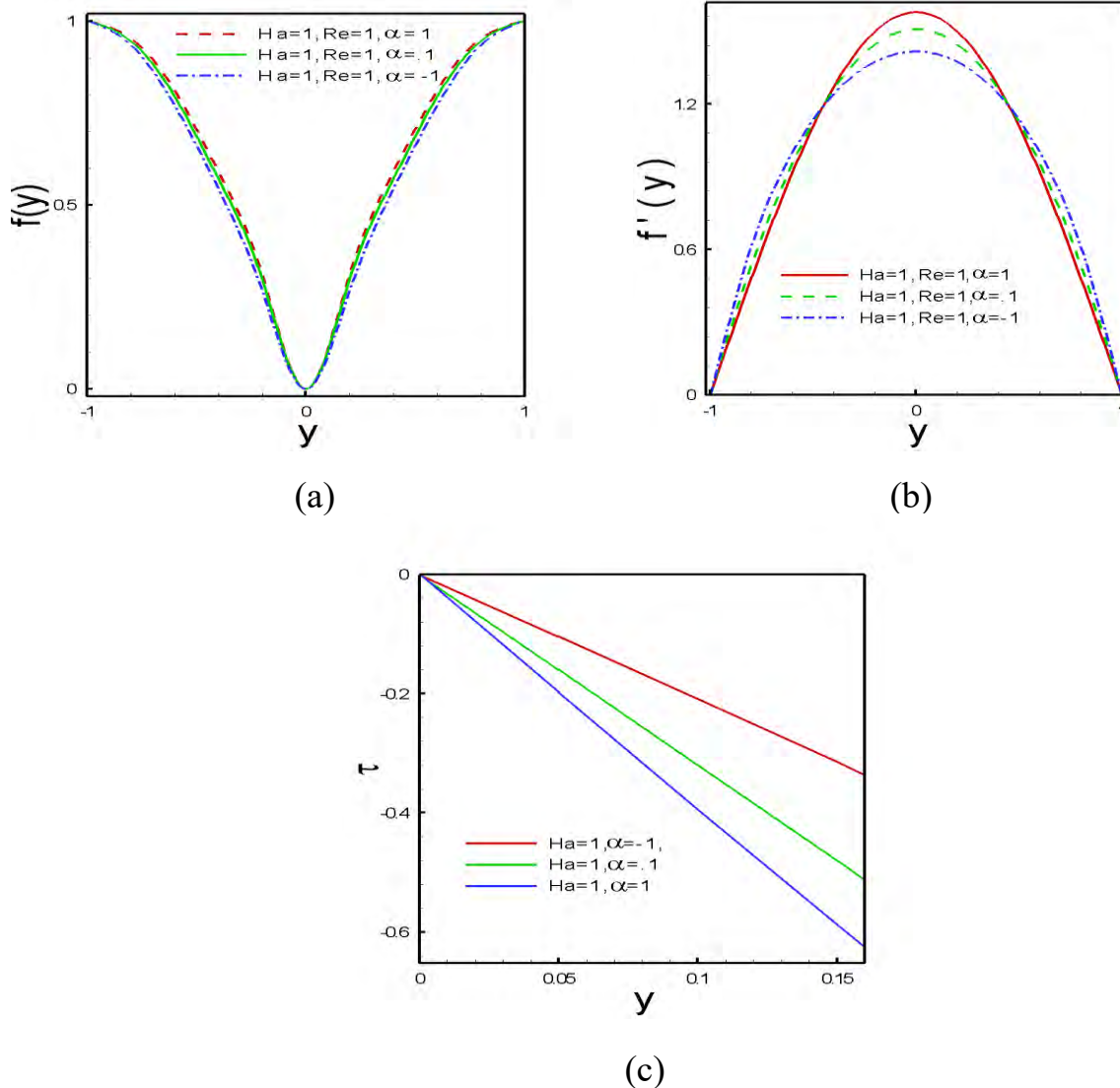


Fig:- 4.7(C)-1(a) Stream function (b) Velocity profile (c) Shear stress for Al_2O_3 -water based nanofluid flow for different value of α , where $\Phi = 0.04$; $Ha = 1$; $Re = 1$.

Fig: (a), Fig: (b) and Fig: (c) show the effects of non-dimensional wall dilation rate α on stream function, fluid velocity and shear stress respectively. The fluid velocity increases along the centerline with the positively increasing values of dimensionless wall dilation rate due to successive expansion of channel width. On the other hand, velocity decreases at the centre of the channel whereas increases near the two plates when α decreases negatively. The absolute value

of shear stress decreases when the non-dimensional wall dilation rate increases. The magnetic field has a significant effect on the velocity profile with the variation of α .

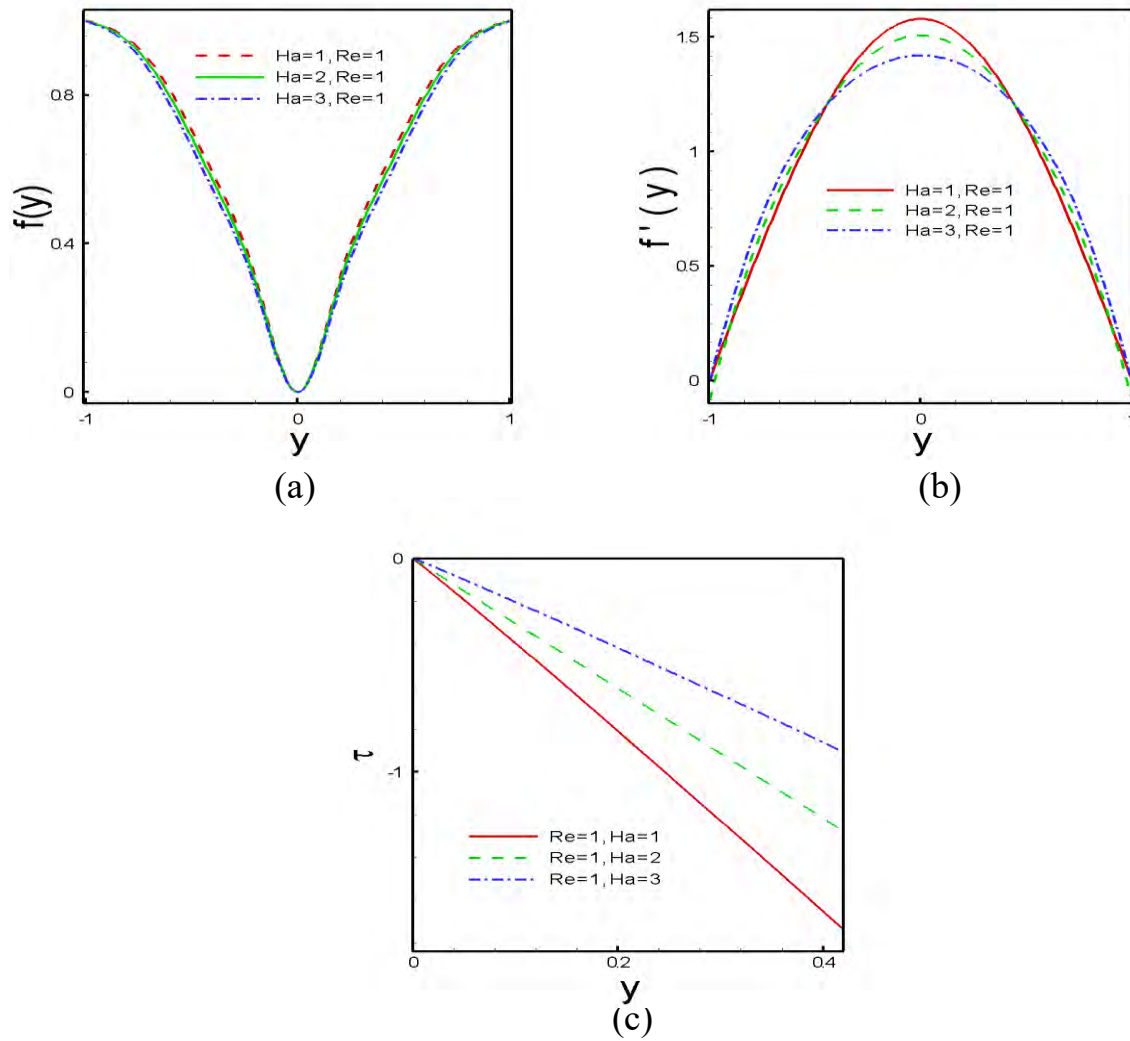


Fig:- 4.7(C)-2(a) Stream function (b) Velocity profile (c) Shear stress for Al_2O_3 - water based nanofluid flow for different value of Ha , where $\alpha = 1$; $Re = 1$; $\Phi = 0.04$.

Fig: (a), Fig: (b) and Fig: (c) show the effect of Hartmann number on stream function, fluid velocity and shear stress respectively. It is seen that velocity at the centre of the channel reduces while enhances around the two plates when Ha increases. The transverse magnetic field opposes the alteration phenomena clearly. Because the variation of Ha leads to the variation of the Lorentz force due to magnetic field and the Lorentz force produces more resistance to the

alternation phenomena. The stream function decreases while Hartmann number Ha increases. The absolute value of shear stress increases when Hartmann number increases.

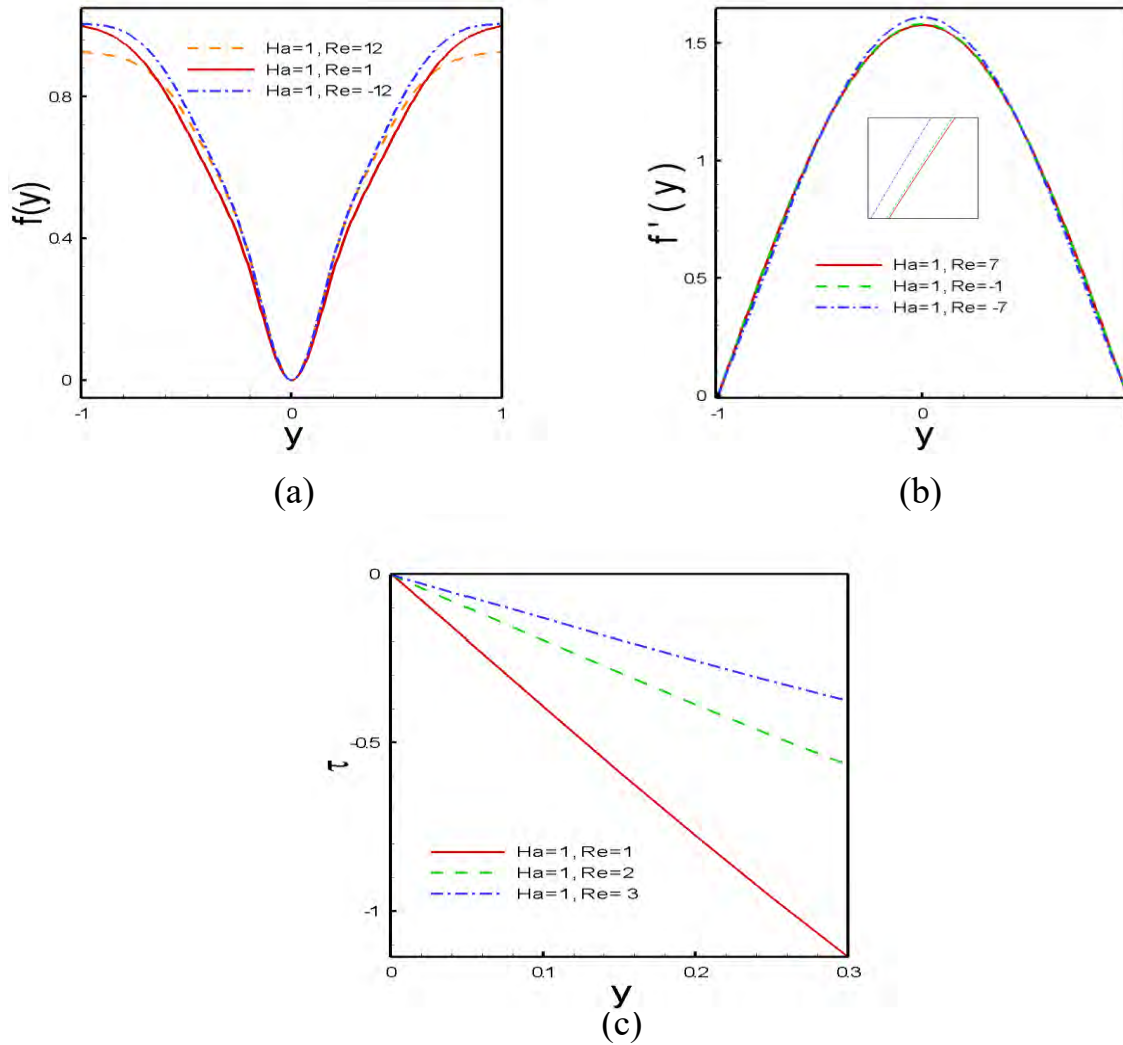


Fig:- 4.7(C)-3 (a) Stream function (b) Velocity profile (c) Shear stress for Al_2O_3 - water based nanofluid flow for different value of Re , where $\alpha = 1$; $Ha = 1$; $\Phi = 0.04$.

Fig: (a), Fig: (b) and Fig: (c) show the effect of Reynolds number on stream function, fluid velocity and shear stress respectively. It can be seen from Fig: (a) and Fig: (b) that fluid centerline velocity reduces while increases near the two walls by the decreasing values of permeation Reynolds number Re . Fig: (c) shows that the absolute value of shear stress increases when Reynolds number increases.

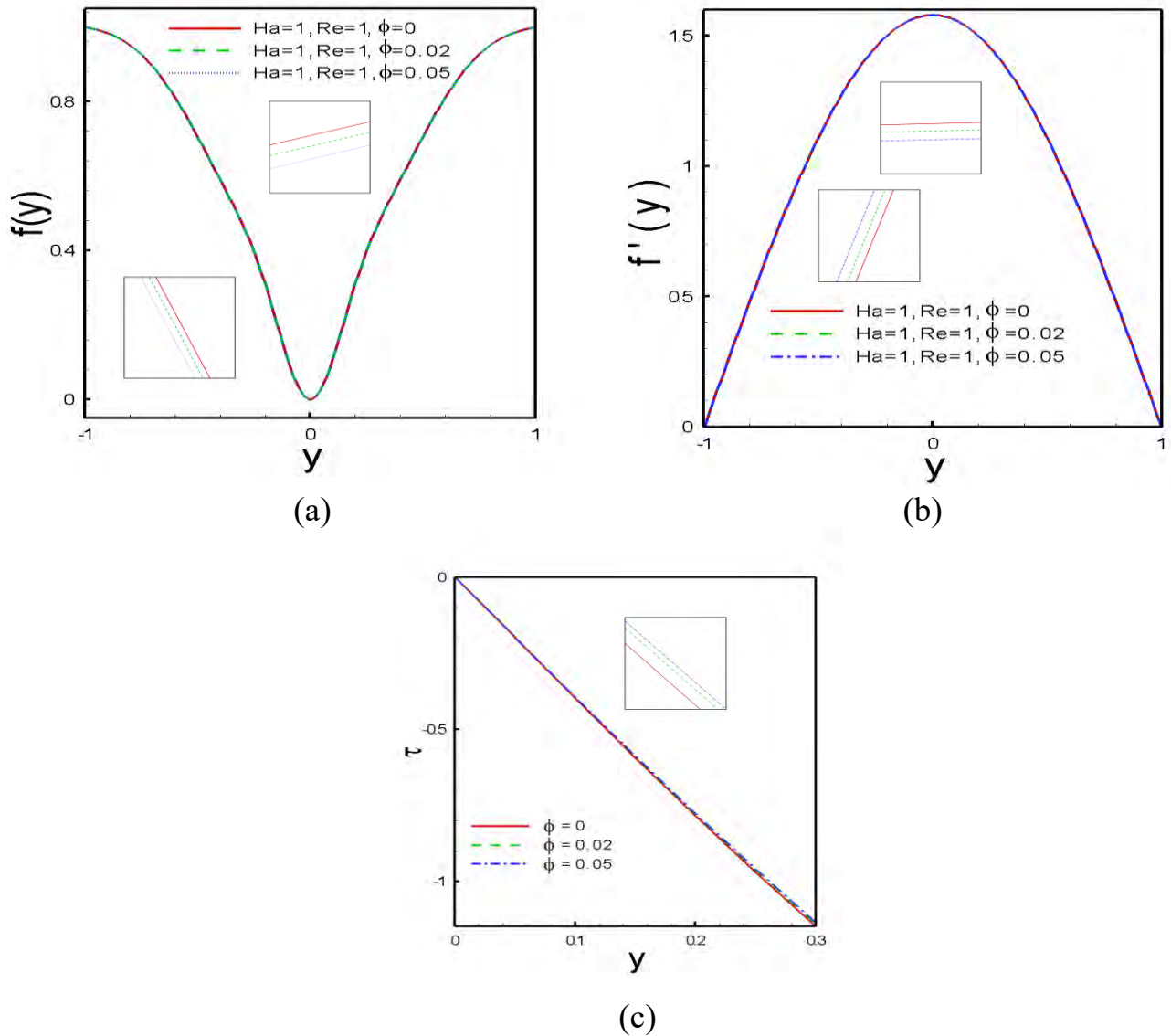


Fig:- 4.7(C)-4 (a) Stream function (b) Velocity profile (c) Shear stress for Al_2O_3 - water based nanofluid flow for different value of Φ , where $\alpha = 1$; $\text{Ha} = 1$; $\text{Re}=1$.

Fig: (a), Fig: (b) and Fig: (c) show the effect of Nanoparticle on stream function, fluid velocity and shear stress respectively. As nanoparticles volume fraction increases, fluid velocity $f'(y)$ at the centre of the channel decreases while increases around the two plates while the value of stream function $f(y)$ decreases. The absolute value of shear stress increases when nanoparticles volume fraction increases.

Table 4.4: Significant differences among different values of Φ for Al_2O_3 -water based nanofluid:

Value of y	Value of $f(y)$			Value of $f'(y)$		
	$\Phi=0.0$	$\Phi=0.02$	$\Phi=0.05$	$\Phi=0.0$	$\Phi=0.02$	$\Phi=0.05$
y = 0	0.000000e-01	0.000000e-01	0.000000e-01	1.578542e+00	1.578419e+00	1.578270e+00
y = ± 0.2	3.104048e-01	3.103822e-01	3.103542e-01	1.499276e+00	1.499181e+00	1.499064e+00
y = ± 0.4	5.897256e-01	5.896816e-01	5.896476e-01	1.270746e+00	1.270724e+00	1.270699e+00
y = ± 0.6	8.104559e-01	8.104158e-01	8.103887e-01	9.188514e-01	9.189182e-01	9.190001e-01
y = ± 0.8	9.515264e-01	9.515040e-01	9.514982e-01	4.810658e-01	4.811629e-01	4.812809e-01
y = ± 1.0	9.999651e-01	9.999601e-01	9.999565e-01	8.482044e-06	6.225546e-06	1.998779e-06

From the table we have that as nanoparticles volume fraction increases, the value of fluid velocity $f'(y)$ at the centre of the channel reduce while enhances around the two plates while the value of stream function $f(y)$ decreases.

Section (D): Stability of MHD fluid (with absence of Nanoparticle) flow through expanding and contracting channel with permeable wall.

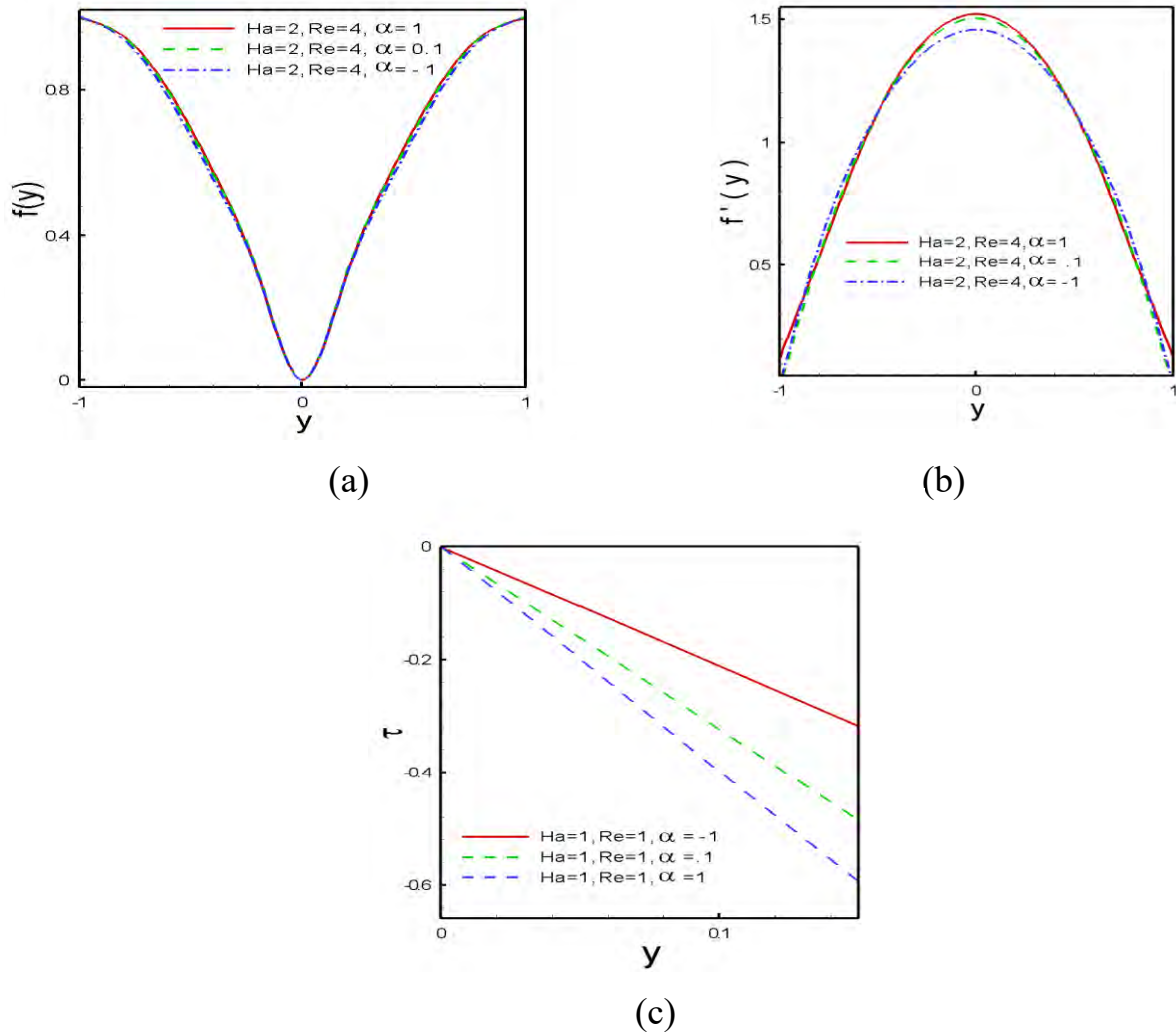
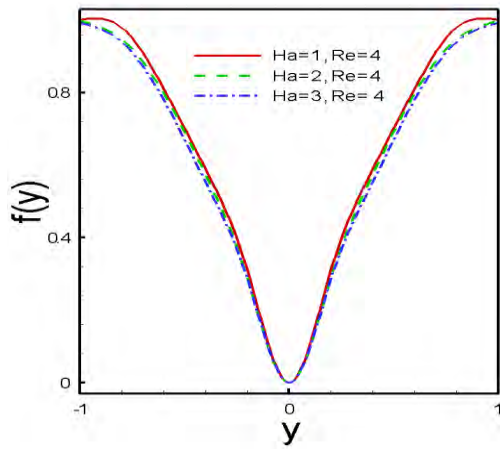
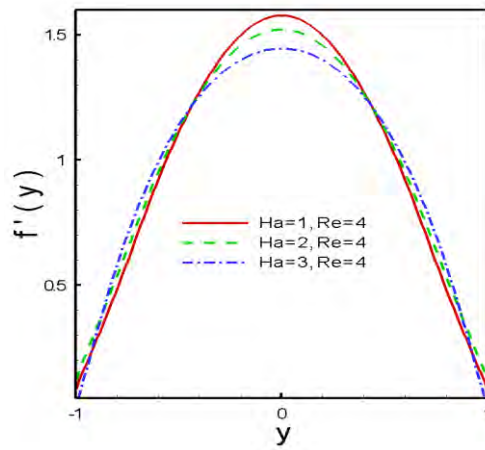


Fig:- 4.7(D)-1 (a) Stream function (b) Velocity profile (c) Shear stress with absence of nanofluid flow for different value of α , where $Ha = 1, 2$; $Re= 1, 4$; $\Phi=0.04$.

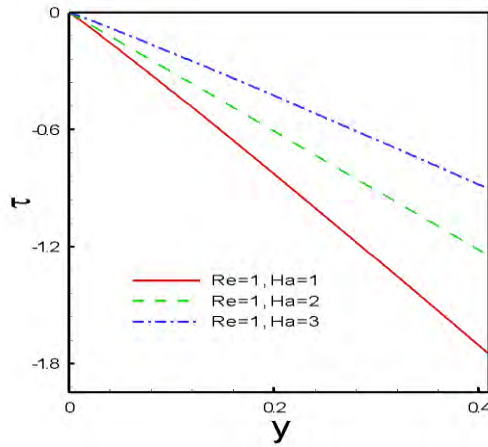
Fig: (a), Fig: (b) and Fig: (c) show the effect of non-dimensional wall dilation rate α on stream function, fluid velocity and shear stress respectively. The fluid velocity increases along the centerline with the positively increasing values of dimensionless wall dilation rate due to successive expansion of channel width. On the other hand, velocity decreases at the centre of the channel whereas increases near the two plates when α decreases negatively. The absolute value of shear stress decreases when the non-dimensional wall dilation rate increases. The magnetic field has a significant effect on the velocity profile with the variation of α .



(a)



(b)



(c)

Fig:- 4.7(D)-2(a) Stream function (b) Velocity profile (c) Shear stress with absence of nanofluid flow for different value of Ha , where $\alpha = 1$; $Re = 1, 4$; $\Phi = 0.04$.

Fig: (a), Fig: (b) and Fig: (c) show the effects of Hartmann number on stream function, fluid velocity and shear stress respectively. It is seen that velocity at the centre of the channel reduces while enhances around the two plates when Ha increases. The transverse magnetic field opposes the alteration phenomena clearly. Because the variation of Ha leads to the variation of the Lorentz force due to magnetic field and the Lorentz force produces more resistance to the alternation phenomena. The stream function is decreased while Hartmann number Ha increases. The absolute value of shear stress increases when Hartmann number increases.

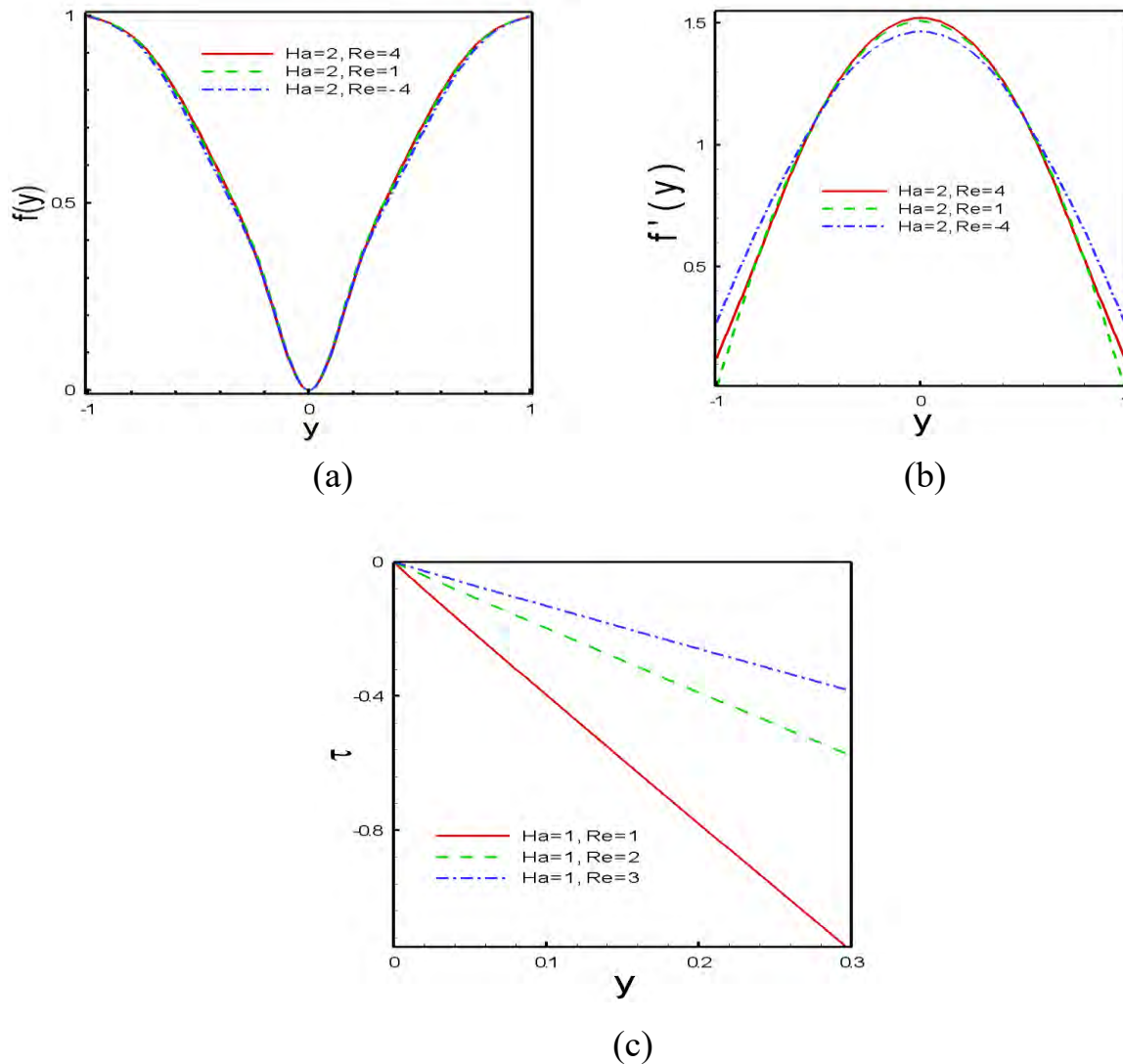


Fig:- 4.7(D)-3 (a) Stream function (b) Velocity profile (c) Shear stress with absence of nanofluid flow for different value of Re , where $\alpha = 1$; $Ha= 1, 2$; $\Phi=0.04$.

Fig: (a), Fig: (b) and Fig: (c) show the effect of Reynolds number on stream function, fluid velocity and shear stress respectively. It can be seen from Fig: (a) and Fig: (b) that fluid centerline velocity reduces while increases near the two walls by the decreasing values of permeation Reynolds number Re . Fig: (c) shows that the absolute value of shear stress increases when Reynolds number increases.

Section (E): Comparison of Stability for Different MHD Nanofluid Flow through Expanding or Contracting Channel with Permeable Walls.

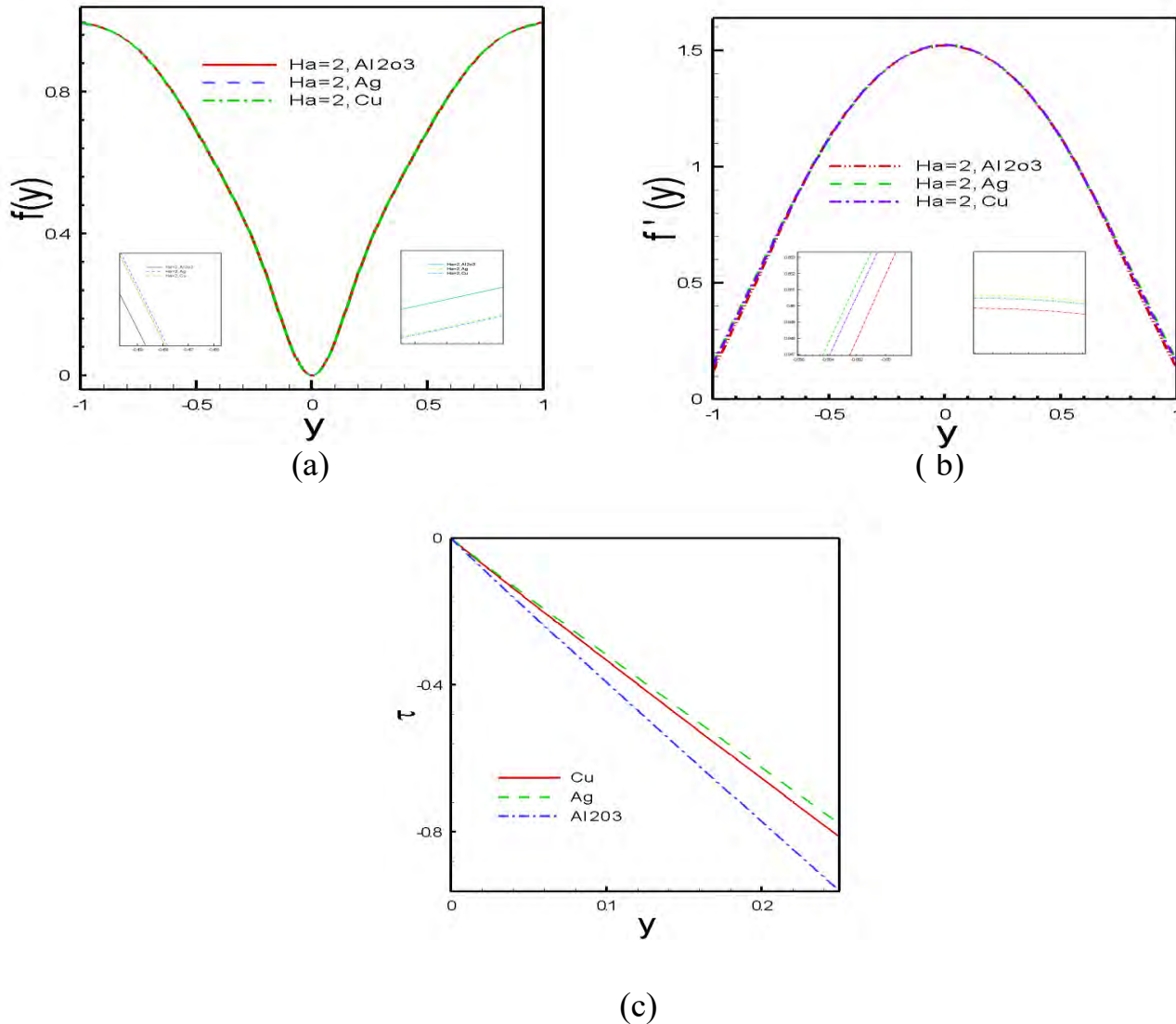


Fig:- 4.7(E)(a) Stream function (b) Velocity profile (c) Shear stress for different nanofluid flow, where $\alpha = 1$; $Ha= 1, 2$; $Re=1, 4$; $\Phi=0.04$.

The effect of different nanoparticles volume fraction on stream function, velocity profile and shear stress are noticed in Fig: (a), Fig: (b) and Fig: (c). They show that the Ag-nanoparticles produce larger horizontal velocity near the walls. Moreover, Cu-nanoparticles enhance centerline velocity. It shows that the absolute value of shear stress is high for Ag and low for Al₂O₃.

Table 4.5: Significant comparison of stability for different MHD nanofluid:

Value of y	Value of $f(y)$			Value of $f'(y)$		
	Cu	Ag	Al ₂ O ₃	Cu	Ag	Al ₂ O ₃
y = 0	0.000000e-01	0.000000e-01	0.000000e-01	1.521615e+00	1.578429e+00	1.578419e+00
y = ± 0.2	2.878144e-01	3.103832e-01	3.103822e-01	1.457512e+00	1.499191e+00	1.499181e+00
y = ± 0.4	5.744740e-01	5.896916e-01	5.896816e-01	1.265640e+00	1.270734e+00	1.270724e+00
y = ± 0.6	7.979769e-01	8.104258e-01	8.104158e-01	9.495213e-01	9.189192e-01	9.189182e-01
y = ± 0.8	9.463118e-01	9.515140e-01	9.515040e-01	5.444338e-01	4.811639e-01	4.811629e-01
y = ±1.0	9.967364e-01	9.999611e-01	9.999601e-01	1.601279e-01	6.225556e-06	6.225546e-06

It shows that the value of stream function $f(y)$ and velocity profile $f'(y)$ produces larger horizontal velocity near the walls for Ag-nanoparticles. Moreover, Cu-nanoparticles enhance centerline velocity.

4.8 Bifurcation

Employing the algebraic approximation method to the series (4.5.2) it obtained the dominating singularity behavior of the function $f(y) \approx (\alpha - \alpha_c)^{\frac{1}{2}}$ with $\alpha_c \approx -2.752214$. Figure 4.8 shows the bifurcation diagram of velocity versus α with the effect of Cu-water nanofluid. We say that there is a *simple turning point, fold or a saddle-node bifurcation* at $\alpha = \alpha_c$. It is interesting to notice that there are two solutions branches of velocity when $\alpha > \alpha_c$, one marginal solution when $\alpha = \alpha_c$ and no solution when $\alpha < \alpha_c$, where α_c is the critical value of α for which the solution exists. The stability analysis indicates that the lower solution branch (I) is stable and physically realizable. For different values of ϕ , the upper solution branch (II) is unstable and physically unacceptable shown in Fig: 4.8.

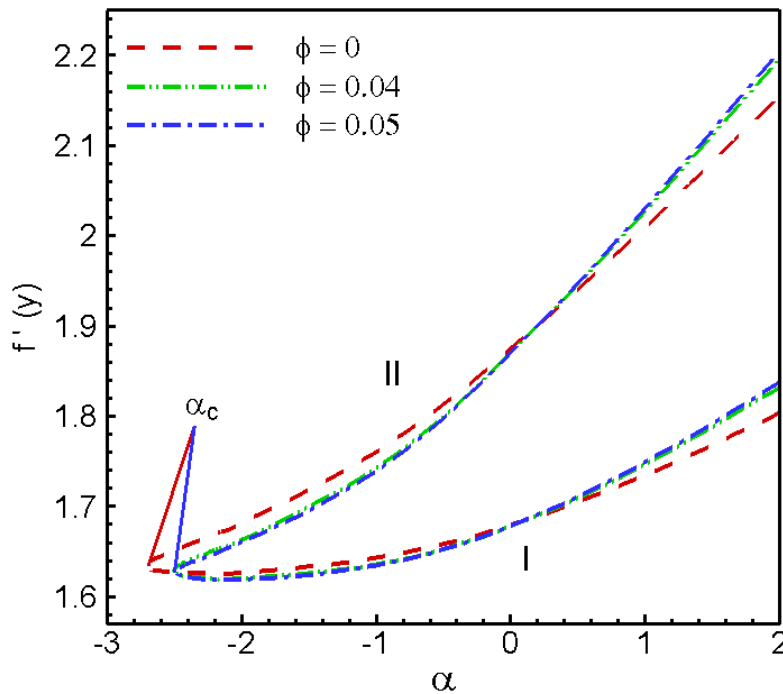


Fig:- 4.8: Bifurcation diagram of velocity at the porous wall for Cu-water based nanofluid.

4.9 Conclusion

The stability of MHD unsteady nanofluids flow through expanding or contracting channel with porous wall in presence of an external magnetic field has been studied numerically. The effects of Hartman number, permeable Reynolds number, non-dimensional wall dilation rate and nanoparticles volume fraction on velocity profile, stream function and shear stress are investigated numerically. The major results of the current study are given as follows.

- As nanoparticles volume fraction increases fluid velocity at the centre of the channel reduces while enhances around the two plates while the value of stream function decreases with presence of Hartmann number.
- The velocity function and stream function is also increased by the increasing values of permeable Reynolds number.
- Ag-nanoparticles accelerate horizontal velocity near the walls whereas Cu-nanoparticles enhance centerline velocity.
- The wall shear stress decreases swiftly by the positive variation of Hartmann number.
- The fluid velocity at the wall has two branches bifurcating at the critical wall dilation rate namely an upper branch and a lower branch. It is found that at the lower solution branch, which is physically acceptable, the value of velocity enhances with the increasing in the nanoparticles volume fraction.

5.1 Conclusion

The thesis has investigated Magnetohydrodynamics (MHD) nanofluid flow through expanding or contracting channel with permeable walls. The governing differential equation for mass momentum is derived according to the physical model of problem. These governing equations with boundary conditions are then made dimensionless by using suitable transformations. The resulting dimensionless nonlinear differential equations are solved numerically using power series with Hermite- Padé approximation method.

A general conclusion of the work is presented below:

- As nanoparticles volume fraction increases, fluid velocity reduces at the centre of the channel and enhances around the two plates while the value of stream function decreases.
- Fluid centerline velocity reduces while increases near the two walls by the decreasing values of permeable Reynolds number.
- The fluid velocity increases along the centerline with the positively increasing values of dimensionless wall dilation rate due to successive expansion of the channel width. On the other hand, velocity decreases at the centre of the channel whereas increases near the two plates when non-dimensional wall dilation rate decreases negatively.
- The Ag-nanoparticles produce larger horizontal velocity near the walls. Moreover, Cu-nanoparticles enhance centerline velocity in absence of magnetic field.
- Effect of Hartmann number on stream function and velocity profiles shows that velocity at the centre of the channel reduces while enhances around the two plates when Hartmann number increases. The transverse magnetic field opposes the alteration phenomena clearly.

- The absolute value of shear stress decreases when the non-dimensional wall dilation rate increases. Moreover, it is also noticed that the wall shear stress decreases rapidly by the positive variation of Hartmann number.
- There are two solutions branches of velocity when $\alpha > \alpha_c$, one marginal solution when $\alpha = \alpha_c = -2.752214$ and no solution when $\alpha < \alpha_c$, where α_c is the critical value of α for which the solution exists. The stability analysis indicates that the lower solution branch (I) is stable and physically realizable. For different values of ϕ , the upper solution branch (II) is unstable and physically unacceptable.

5.2 Possible future works based on this thesis

The present study can be extended by considering the following cases:

- Temperature dependent physical properties like viscosity, Prandtl number with different physics like heat generation, stress work may be considered.
- The study can be considered for three-dimensional flow.
- This work can be extended by considering stretchable, porous wall of the convergent-divergent channel.
- Investigation can be carried out on nanofluids for turbulent flow.

Reference

- [01] A K. Khan, R. Rashid, G. Murtaza, and A. Zahra (2014) “Gold nanoparticles: synthesis and applications in drug delivery,” *Tropical J. of Pharm. Res*13 (7), 116–117.
- [02] Alam, M.S. and M.A.H. Khan, (2010), “Critical behavior of the MHD flow in convergent-divergent channels”, *Journal of Naval Architecture and Marine Engineering*, Vol.7, No.2, pp 83-93.
- [03] Alam, Md.S. (2016), “Numerical study on stability of MagnetoHydrodynamic nanofluid flow through channel”, Ph.D. thesis, Bangladesh University of Engineering & Technology, Dhaka.
- [04] Dauenhauer, J. Majdalani (1999), Unsteady flows in semi-infinite expanding channels with wall injection. AIAA paper, pp. 99-3523.
- [05] Hady, F. Ibrahim, H El- Hawery, and A Abdelhady (2012), “Effect of suction /injection on natural convection boundary layer flow of a nanofluid past a vertical porous plate through a porous medium,” *J. of Mod. Meth. In Numer Math* 3(1), 53–63.
- [06] Hermite (1893), Sur la généralisation des fractions continues algébriques, *Annali di Mathematica Pura e Applicata* 21(2), 289-308.
- [07] H. N. Chang, J.S. Ha, J.K. Park, I.H. Kim, H.D. Shin(1989) , Velocity field of pulsatile flow in a porous tube, *J. Biomech.*22 1257-1262.
- [08] H. Padé (1892), Sur la representation approchée d’une fonction pour des fractions rationnelles, *Ann. Sci. École Norm. Sup. Suppl* 9, 1-93.
- [09] J. Majdalani, C. Zhou, and C. A. Dawson (2002), “Two–dimensional viscous flow between slowly expanding, contracting walls with weak permeability,” *J. of Biomech.*35, 1399–1403.
- [010] Kashif, M.Z. Akbar, M.F. Iqbal, and M. Ashraf (2014), “Numerical simulation of heat and mass transfer in unsteady nanofluid between two orthogonally moving porous coaxial disks,” *AIP Advances*4, 107713 10.1063/1.489747.
- [011] K. Zaimi, A Ishak, and I. Pop, (2014), “Unsteady flow due to a contracting cylinder in a nanofluid using Buongiorno’s model,”*Inter. J. of Heat and Mass Transfer* 68, 509–513.
- [012] M.A.H. Khan (2001), “Singularity analysis by summing power series”, Ph.D. Thesis, University of Bristol, U.K.

- [013] M.A.H. Khan (2002), High-Order Differential Approximants, *Journal of Computational and Applied Mathematics* 149, 452-468.
- [014] M. Fakour, A. Vahabzadeh, D.D. Ganji, and M. Hatami (2015), “Analytical study of micropolar fluid flow and heat transfer in a channel with permeable walls,” *J. of Mol. Liquid* pages-7.
- [015] Malvandi and D.D. Ganji (2104), “Magnetic field effect on nanoparticles migration and heat transfer of water / alumina nanofluid in a channel,” *J. of Magn. & Magnet. Materials*362, 172–179.
- [016] M. Jashim, O.Uddin, A. Beg, and A. I. MD (2014), “Ismail, Mathematical modeling of radiative hydromagnetic thermo solute nanofluid convection slip flow in saturated porous media,” *Hindawi Pub. Corp.* pages-11.
- [017] M. Hatami, J. Hatami, and D. D. Ganji (2014), “Computer simulation of MHD blood conveying gold nanoparticles as a third grade non Newtonian nanofluid in a hollow porous vessels,” *Computer Method and Program in Biomedicine* 113,632–641.
- [018] M. Hatami, R. Nouri, and D.D. Ganji (2013), “Forced convection analysis for MHD Al_2O_3 -water nanofluid flow over a horizontal plate,” *J. of Mol. Liquids*187 (0), 294–301.
- [019] M. Hatami and D. D. Ganji (2013), “Heat transfer and nanofluid flow in suction and blowing process between parallel disks in presence of variable magnetic field,” *J. Mol. Liquids*190(0), 159–168.
- [020] M. Hatami, A. Hassan pour, and D. D. Ganji(2013), “Heat transfer study though porous fins (Si_3N_4 and AL) with temperature dependent heat generation,” *Energy Conver. Manag*74, 9–16.
- [021] *M. Hatami, S.A.R. Sahebi, A.Majidian, M. Sheikholeslami, D. Jing, G. Domairry, Numerical analysis of nanofluid flow conveying nanoparticles through expanding and contracting gaps between permeable walls. Journal of Molecular Liquids 212 (2015) 785-791.*
- [022] M. K. Rahman, Md. S. Alam. M.A.H.Khan, “*Stability on Magnetohydrodybamics Nanofluid flow through expanding or contracting channel with permeable walls.*” *Procedia Engineering* 194 (2017) 487 – 493.

- [023] M.M. Rashidi, N. Vishnu Ganesh, A.K. Abdul Hakeem, and B. Ganga (2014), “Buoyancy effect on MHD flow of nanofluid over a stretching sheet in the presence of thermal radiation,” *J. of Mol. Liquids*198, 234–238.
- [024] M. Sheikholeslami, M. Hatami, and D. D. Ganji (2013), “Analytical investigation of MHD nanofluid flow in a semi-porous channel,” *Powder Technology*, pages-10.
- [025] M. Sheikholeslami, M. Gorji-Bandpy, R. Ellahi, M. Hassan, and S. Soleimani (2014), “Effects of MHD on Cu water nanofluid flow and heat transfer by means of CVFEM,” *J. Magn. & Magnet. Mater.* 349(0), 188–200.
- [026] M. Sheikholeslami, M. Gorji-Bandpy, and D. D. Ganji (2012), “Magnetic field effects on natural convection around a horizontal circular cylinder inside a square enclosure filled with nanofluid,” *Int. Commun. Heat Mass Transfer*39 (7), 978–986.
- [027] M. Sheikholeslami, M. Gorji-Bandpy, D. D. Ganji, and S. Soleimani (2014), “Heat flux boundary condition for nanofluid filled enclosure in presence of magnetic field,” *J. of Mol. Liquids*193, 174–184.
- [028] M. Sheikholeslami, M. G-Bandpy, D. D. Ganji, and S. Soleimani(2012), “Effect of a magnetic field on natural convection in an enclosure between a circular and sinusoidal cylinder in the presence of magnetic field,” *Int. Commun. Heat Mass Transfer* 39(9), 1435–1443.
- [029] M.Sheikholeslami, M. G-Bandpy, D. D. Ganji, P. Rana, and S Soleimani (2014), “Magnetohydrodynamics free convection of Al_2O_3 –water nanofluid considering thermophoresis and Brownian motion effects,” *Computers & Fluids* 94, 147–160.
- [030] M. Sheikholeslami, D. D. Ganji, M .Y .Javed, and R. Ellahi (2015), “Effect of thermal radiation on magnetohydrodynamics nanofluid flow and heat transfer by means of two phase model,” *J. of Magna.& Magnet. Materials*374, 36–43.
- [031] M.M. Rashidi, S. Abelman, N. Freidooni Mehr (2013), Entropy generation in steady MHD flow due to a rotating porous disk in a nanofluid. *Int. J. Heat Mass transf.* 62, 515-525.
- [032] Nield and A. Bejan (2006), *Convection in Porous Media*, 4th ed. (Springer, New York), pp. 1–29.

- [033] N.C. Sacheti (2003), “Application of Brinkman model in viscous incompressible flow through a porous channel,” *J. of Nume. Method for Heat and Fluid Flow* 13(7), 830–848.
- [034] P. G. Drazin, and Y. Tourigny (1996), Numerically study of bifurcation by analytic continuation of a function defined by a power series, *SIAM Journal of Applied Mathematics* 56, 1-18.
- [035] R.A. Mahdi, H.A Mohammed, K. M. Munisamy, and N. H. Saied(2015), “Review of convection heat transfer and fluid flow in porous media with nanofluid,” *Renewable and Sustainable Energy Reviews*41, 715–734.
- [036] Rahman, M. M., (2004), “A new Approach to Partial Differential Approximants”, M. Phil thesis, Bangladesh University of Engineering & Technology, Dhaka.
- [037] S. Berman (1953), Laminar flow in channels with porous wall. *J. Appl. Phys.* 24 1232-1235.
- [038] S.K.Das and S.U.S.Choi (2007), *Nanofluid: science and technology* (Wiley, New-Jersey).
- [039] S.U.S.Choi (1995), “Enhancing thermal conductivity of fluids with nanoparticles,” ASME Publication FED 231/ MD 66, 99–105.
- [040] S. Uchida and H. Aoki (1977), “Unsteady flows in a semi-infinite contracting or expanding pipe,” *J. of Fluid Meach.*82, 371–387.
- [041] T. Hayat, M Rashid, M Imtiaz, and A. Alsaedi (2015), “Magnetohydrodynamics (MHD) flow of Cu-water nanofluid due to a rotating disk with partial slip,” *AIP Advances*5, 067169 doi: 10.1063/1.4923380.
- [042] T. Hayat, M. U Qureshi, and Q. Hussain (2009), “Effect of heat transfer on the peristaltic flow of an electrically conducting fluid in a porous space,” *Appl. Math. Modell.*33 (4), 1862–1873.
- [043] X-Q, Wang, A.S. Mujumdar (2007), “Heat transfer characteristic of Nanofluid:” A review, *Int. J. Therm. Sci.* 46, 1-19.
- [044] Y. Z. Boutros, M.B. Abd-el-Malek, N.A. Badran, H.S. Hasan (2006), “Lie group method for unsteady flows in a semi-infinite expanding or contracting pipe with injection or suction trough a porous wall”. *J. Comput. Appl. Math.* 192(2) 465-494.

